THIS REPORT HAS BEEN DELIMITED
AND CLEARED FOR PUBLIC RELEASE
UNDER DOD DIRECTIVE 5200.20 AND
NO RESTRICTIONS ARE IMPOSED UPON
ITS USE AND DISCLOSURE.

DISTRIBUTION STATEMENT A

APPROVED FOR PUBLIC RELEASE;
DISTRIBUTION UNLIMITED.

UNCLASSIFIED

Reproduced by the

ARMED SERVICES TECHNICAL INFORMATION AGENCY
ARLINGTON HALL STATION
ARLINGTON 12, VIRGINIA

DECLASSIFIED
DOD DIR 5200.9

UNCLASSIFIED

Armed Services Technical Information Agency

Because of our limited supply, you are requested to return this copy WHEN IT HAS SERVED YOUR PURPOSE so that it may be made available to other requesters. Your cooperation will be appreciated.

AD 41462

NOTICE: WHEN GOVERNMENT OR OTHER DRAWINGS, SPECIFICATIONS OR OTHER DATA ARE USED FOR ANY PURPOSE OTHER THAN IN CONNECTION WITH A DEFINITELY RELATED GOVERNMENT PROCUREMENT OPERATION, THE U. S. GOVERNMENT THEREBY INCURS NO RESPONSIBILITY, NOR ANY OBLIGATION WHATSOEVER; AND THE FACT THAT THE GOVERNMENT MAY HAVE FORMULATED, FURNISHED, OR IN ANY WAY SUPPLIED THE SAID DRAWINGS, SPECIFICATIONS, OR OTHER DATA IS NOT TO BE REGARDED BY IMPLICATION OR OTHERWISE AS IN ANY MANNER LICENSING THE HOLDER OR ANY OTHER PERSON OR CORPORATION, OR CONVEYING ANY RIGHTS OR PERMISSION TO MANUFACTURE, USE OR SELL ANY PATENTED INVENTION THAT MAY IN ANY WAY BE RELATED THERETO.

Reproduced by

DOCUMENT SERVICE CENTER

KNOTT BUILDING, D[illegible]

NOTICE: THIS DOCUMENT CONTAINS INFORMATION AFFECTING THE NATIONAL DEFENSE OF THE UNITED STATES WITHIN THE MEANING OF THE ESPIONAGE LAWS, TITLE 18, U.S.C., SECTIONS 793 and 794. THE TRANSMISSION OR THE REVELATION OF ITS CONTENTS IN ANY MANNER TO AN UNAUTHORIZED PERSON IS PROHIBITED BY LAW.

Copy No. 00001

WIDE-APERTURE DISTRIBUTION OF NARROW-APERTURE RADIO DIRECTION FINDING SYSTEMS WITH OPTICAL SUPERPOSITION OF UNIT BEARING INDICATIONS

Technical Report No. 10
1 August 1950

N6-ori-71 Task XV
ONR Project No. 076 161

Supervisors

A. D. Bailey E. C. Jordan H. D. Webb

Research Associates and Assistants

J. M. Anderson
R. W. Annis
R. H. Brunner
R. A. Campbell
R. H. DuHamel
V. J. Fowler
E. C. Hayden
C. T. A. Johnk
B. D. Kirkwood
R. E. Lepic
T. R. O'Meara
D. E. Royal
N. Yaru

Approved by: A D Bailey
A. D. Bailey

Approved by: H D Webb
H. D. Webb

"This document contains information affecting the national defense of the United States within the meaning of the Espionage Act, 50 U.S.C., 31 and 32, as amended. Its transmission or the revelation of its contents in any manner to an unauthorized person is prohibited by law. Reproduction of this matter in any form by other than Naval activities is not authorized except by specific approval of the Secretary of the Navy."

RADIO DIRECTION FINDING RESEARCH LABORATORY
DEPARTMENT OF ELECTRICAL ENGINEERING
UNIVERSITY OF ILLINOIS
URBANA, ILLINOIS

DISTRIBUTION LIST FOR TECHNICAL REPORT NO. 10

	Copy No.
Chief of Naval Research Attention: Electronics Branch Code 427 Office of Naval Research Washington 25, D. C. (2 copies)	1-2
Director, Naval Research Laboratory Anacostia, D. C. (5 copies)	3-7
Naval Research Laboratory Attention: Technical Information Officer Washington 25, D. C. (9 copies)	8-16
Director, Special Devices Center Office of Naval Research Sands Point, Port Washington Long Island, N. Y. (1 copy)	17
Commanding Officer Office of Naval Research Branch Office America Fore Building 844 North Rush Street Chicago, Illinois (2 copies)	18-19
Chief of Naval Operations (Op 20-2) Navy Department Washington 25, D. C. (2 copies)	20-21
Chief of Naval Operations (Op 20-FZ) Navy Department Washington 25, D. C. (1 copy)	22
Chief of Naval Operations (Op-413-Z) Navy Department Washington 25, D. C. (1 copy)	23
Chief of Naval Operations (Op 50-z) Navy Department Washington 25, D. C. (1 copy)	24
Chief of the Bureau of Aeronautics (R-7) Navy Department Washington 25, D. C. (1 copy)	25
Chief of the Bureau of Aeronautics (El-3) Washington 25, D. C. (1 copy)	26
Chief of the Bureau of Aeronautics El-91 Navy Department Washington 25, D. C. (1 copy)	27
Chief of the Bureau of Aeronautics (El-33) Washington 25, D. C. (1 copy)	28
Chief of the Bureau of Aeronautics (El-4) Washington 25, D. C. (1 copy)	29
Chief of Naval Operations (Op-413-B) Navy Department Washington 25, D. C. (1 copy)	30
Chief of the Bureau of Ships (910) Navy Department Washington 25, D. C. (1 copy)	31
Chief of the Bureau of Ships (913) Navy Department Washington, D. C. (1 copy)	32

	Copy No.
Chief of the Bureau of Ships (925D) Navy Department Washington 25, D. C. (1 copy)	33
Commanding General Air Materiel Command (TSE[illegible]) Wright-Patterson Air Force Base Dayton, Ohio (2 copies)	34-35
Naval Liaision Officer Signal Corps Engineering Laboratory (CSL) Fort Monmouth, New Jersey (2 copies)	36-37
Signal Corps Engineering Laboratory Bradley Beach, New Jersey (2 copies)	38-39
U. S. Naval Academy PG School, Electrical Engineering Department, Annapolis, Maryland (1 copy)	40
Commanding Officer U. S. Navy Office of Naval Research Branch Office 495 Summer Street Boston 10, Massachusetts (1 copy)	41
Commanding Officer U. S. Navy Office of Naval Research Branch Office 346 Broadway New York 13, N. Y. (1 copy)	42
Director, U.S. Naval Electronics Laboratory San Diego, California (2 copies)	43-44
Chief, Bureau of Ships Code 903 Navy Department Washington 25, D. C. (1 copy)	45

	Copy No.
Chief of the Bureau of Ships (911) Navy Department Washington 25, D. C. (1 copy)	46
Chief of the Bureau of Ships (920) Navy Department Washington 25, D. C. (1 copy)	47
Chief of the Bureau of Ships (930) Navy Department Washington 25, D. C. (1 copy)	48
Chief Signal Officer U. S. Army, Code Sig TA2S Pentagon Building Washington 25, D. C. (1 copy)	49
Central Radio Propagation Laboratory U. S. Bureau of Standards Washington, D. C. (2 copies)	50-51
Commanding Officer U. S. Navy Office of Naval Research Branch Office 801 Donahue Street San Francisco 5, California (1 copy)	52
Assistant Naval Attache for Research American Embassy Navy 100 c/o Fleet Post Office New York, N. Y. (1 copy)	53
Commander Operational Development Force Fleet Post Office New York, N. Y. (1 copy)	54
Electrical Engineering Research Laboratory Attention: Dr. A. W. Straiton University of Texas Austin 12, Texas (1 copy)	55

	Copy No.
Commanding Officer Office of Naval Research Branch Office 1030 East Green Street Pasadena 1, California (1 copy)	56
Bureau of Aeronautics General Representative, USN Central District Wright-Patterson Air Force Base Dayton, Ohio "For transmittal to Air Materiel Command" (3 copies)	57-59

TABLE OF CONTENTS

I. ABSTRACT

A system is proposed and analyzed for optically combining the bearing information from a wide-aperture distribution of narrow-aperture Watson-Watt dual-channel direction finders in such a way as to use the envelope of a series of ellipses to resolve the directions of arrival of two or more radio waves having the same frequency.

Photographs and diagrams are given illustrating a laboratory model of a distribution of seven Watson-Watt systems. Photographs of the bearing information from this system illustrate the effects of varying system diameter, time phase difference, relative magnitude, and angular separation with two incoming waves. The photographs are discussed as to the merits of various bearing reading techniques.

It is demonstrated that seven Watson-Watt units, circularly distributed and connected so as to have optically superimposed bearing indications, can form a system capable of completely resolving the directions of arrival of two signals under a majority of conditions. It is further shown that with a sufficient number of Watson-Watt units, the directions of arrival of more than two incoming signals can be reduced.

II. INTRODUCTION

One of the objectives of the radio direction finding research program at the University of Illinois has been the investigation of wide-aperture radio direction finding systems which have potentialities toward overcoming the bearing errors caused by wave interference effects resulting from the presence of several rather than one arriving wave.

One of the most promising general techniques for synthesizing wide-aperture systems lies in the combination of bearing information from a limited space distribution of narrow-aperture systems. Practical considerations suggest that wide-aperture systems using existing radio direction finders be thoroughly investigated. The space distribution must be wide aperture in the sense of being distributed over several wavelengths, yet limited to the extent that each system must give the same bearing under ideal conditions (as opposed to wide base systems used to obtain a bearing fix.) The letters WADONAS will be used to designate such a Wide-Aperture Distribution Of Narrow-Aperture Systems in this report.

There are, at least, two general techniques for utilizing the bearing information from a WADONAS. The first technique is combining the bearing information electrically in such a way that the combined signal (or signals) is capable of giving a sort of average bearing on an indicator. Several possible techniques for accomplishing this combination and bearing presentation are discussed in Technical Report No. 9 of of this project, Section V c.

The second combination technique is an optical combination or superposition. The bearings of the individual direction finders are superimposed (optically) in such a way as to obtain a better degree of bearing resolution than any single system would normally offer. Selecting the strongest bearing or an 'eye average' of the strongest bearings (in effect a diversity technique) is one method of optical 'combination'. A more refined technique is to use the envelope of the bearing presentations and this is the scheme with which this report is concerned.

The individual systems making up the WADONAS are dual-channel cathode-ray or Watson-Watt systems. Since these systems are instantaneous in their operation, the WADONAS is also. Hence, such a WADONAS is ideally suited for direction finding on flash ('squash') transmissions. In order to better explain the principles underlying the use of the combination technique explained in Section V, the basic principles and equations underlying the operating of a single Watson-Watt direction finder are reviewed in Section IV.

Since in multipath sky-wave transmission the incoming signals will be arriving from nearly the same horizontal angle, much of the data in this report was obtained for the conditions of 5° and 10° azimuthal separation between signals which are important practical cases.

III. LIST OF SYMBOLS

h	relative magnitude of the weaker of two incoming signals compared to the stronger.
φ	time phase difference between two interfering signals at the center of a composite system.
φ_n	time phase difference between two interfering signals at the center of the nth Watson-Watt direction finder making up a distributed system.
α	angle of arrival of the strongest wave measured counter-clockwise from the x axis.
β	angle of arrival of an interfering signal measured counter-clockwise from the direction of arrival of the desired signal.
e_n	voltage induced in the nth Adcock antenna.
e_x	differential antenna voltage, east-west antennas.
e_y	differential antenna voltage, north-south antennas.
d_x	x deflection on oscilloscope screen.
d_y	y deflection on oscilloscope screen.
$Z = d_x + j\,d_y$	oscilloscope deflection as a complex number.
θ_e	indication error for a Watson-Watt system with two incoming waves.
ψ	shift in time phase difference between time phase difference at the center of a distributed system and time phase difference φ_n at the center of a unit system.
ψ_{max}	absolute maximum of ψ for any position on a circle of the unit system.
Γ_m	polar angle between a unit system and a direction of arrival of a signal.
A	sizing factor for oscilloscope trace. Includes electric field strength at antennas, complex amplifier gain, etc.
K	equal to $\frac{2\pi}{\lambda}$.
B_n	bearing nth signal measured clockwise from north.
λ	wavelength of the radio frequency signal.
r	radius of circular WADONAS

IV WATSON-WATT RDF UNDER SIGNAL CONDITIONS

A. Effect of Field Caused by One Signal

Figure 1 depicts the geometry involved in this discussion. Assume a wave propagating in the $-y'$ direction and given by

$$E = E_m \sin (\omega t + Ky'). \tag{1}$$

Assume that the Adcock antenna masts placed at points 1, 2, 3, and 4 are electrically identical and so have equal pickup factors. Assume that the maximum value of the field strength, E_m, is the same at all these points and is equal to that at point 0. Then, one can write

$$e_1 = e_o \sin (\omega t + r\ K \cos \alpha) \tag{2}$$

$$e_2 = e_o \sin (\omega t - r\ K \cos \alpha) \tag{3}$$

$$e_3 = e_o \sin [\omega t + r\ K \cos (\frac{\pi}{2} - \alpha)] \tag{4}$$

$$e_4 = e_o \sin [\omega t - r\ K \cos (\frac{\pi}{2} - \alpha)] \tag{5}$$

where $e_o \sin \omega t$ is the voltage which would be present at an antenna at point 0, the center of the array. Let the antennas be differentially connected to produce

$$e_x = e_1 - e_2 \tag{6}$$

and

$$e_y = e_3 - e_4. \tag{7}$$

Then

$$e_x = e_o \sin(\omega t + r\ K \cos \theta) - e_o \sin(\omega t - r\ K \cos \alpha)$$

$$= 2e_o \sin(r\ K \cos \alpha) \cos \omega t \tag{8}$$

and similarly,

$$e_y = 2e_o \sin [r\ K \cos(\frac{\pi}{2} - \alpha)] \cos \omega t$$

$$= 2e_o \sin (r\ K \sin \alpha) \cos \omega t. \tag{9}$$

Since

$$\sin(r\ K \cos \alpha) = 2 \sum_{n=0}^{\infty} (-1)^n J_{2n+1}(rK) \cos(2n+1)\alpha \tag{10}$$

where

$$J_m(rK) = \frac{(rK)^m}{2^m m!} (1 - \frac{(rK)^2}{2(2m+2)} + \frac{(rK)^4}{2 \cdot 4(2m+2)(2m+4)} \cdots). \tag{11}$$

For (rK) small with respect to a wavelength one can approximate

$$\sin(rK \cos \alpha) \cong rK \cos \alpha \tag{12}$$

and by the same license

$$\sin(rK \sin \alpha) \cong rK \sin \alpha. \tag{13}$$

It is then nearly true that

$$e_x = 2e_o\ rK \cos \alpha \cos \omega t \tag{14}$$

$$e_y = 2e_o\ rK \sin \alpha \cos \omega t. \tag{15}$$

If e_x and e_y are amplified and applied to the x and y plates, respectively, of an oscilloscope, the deflection of the beam from the center is given by

$$d_x = K_x\ e_o\ rK \cos \alpha \cos \omega t \tag{16}$$

$$d_y = K_y\ e_o\ rK \sin \alpha \cos \omega t.$$

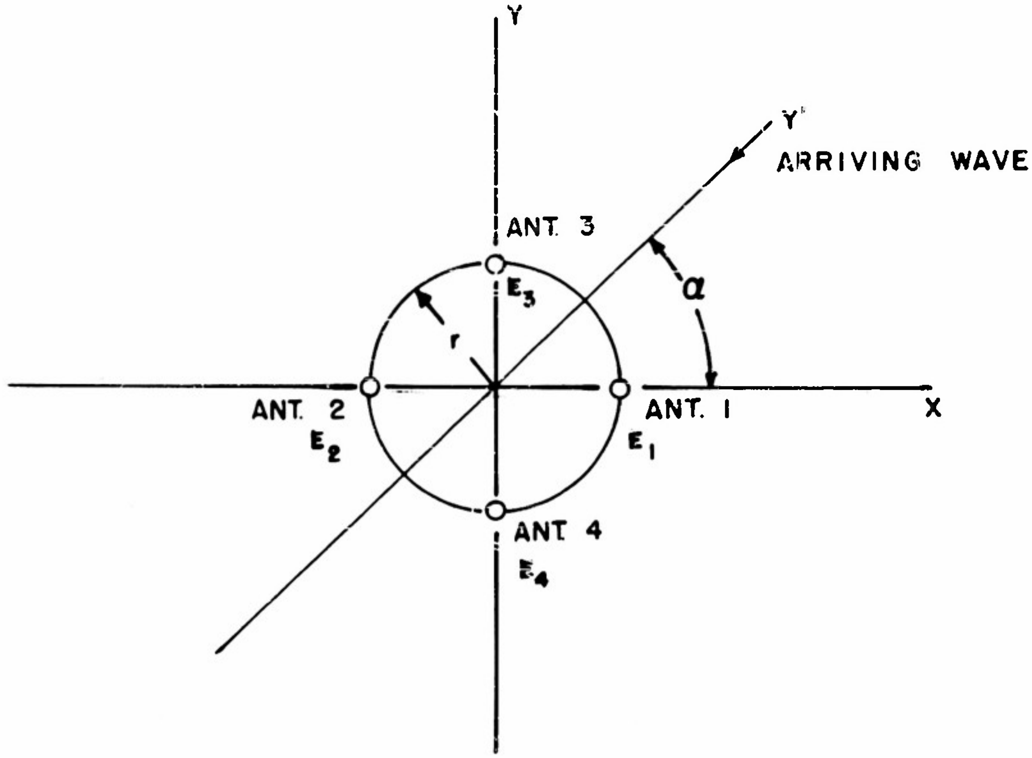

FIGURE 1

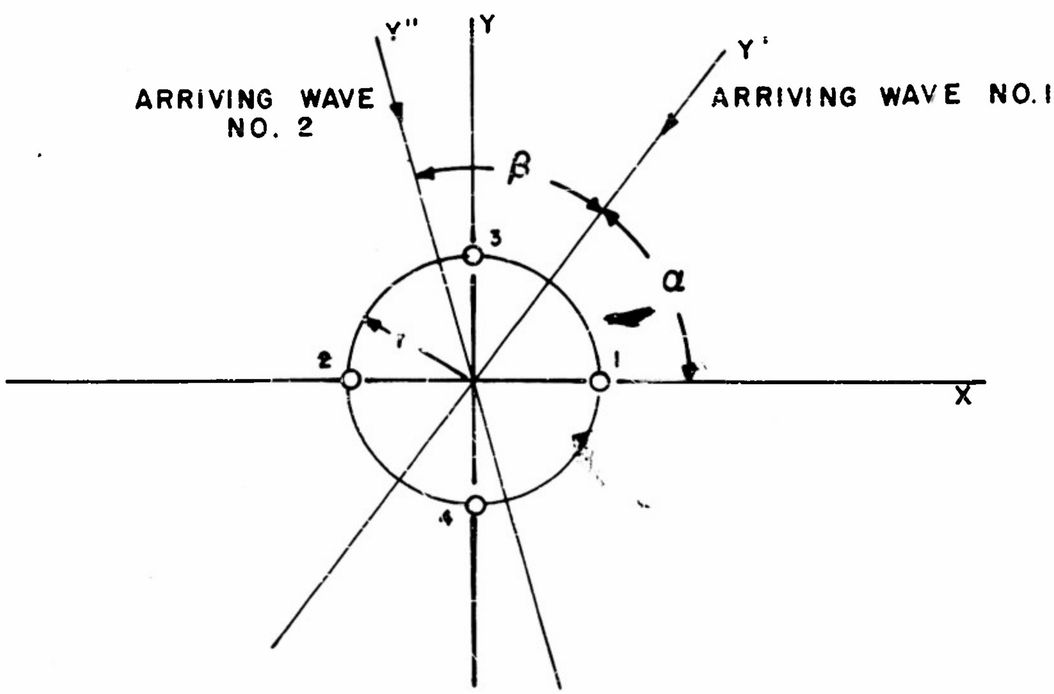

FIGURE 2

Complex notation affords a convenient way to express the above. If a one-to-one correspondence between points on the oscilloscope face and points in the complex Z plane be set up, one has, allowing $d_x = X$ and $d_y = Y$

$$Z = X + jY = K_x e_o r K \cos\alpha \cos\omega t + jK_x e_o r K \sin\alpha \cos\omega t. \tag{18}$$

Adjust $K_x = K_y$ so that

$$d_{x\,max} = d_{y\,max} = A. \tag{19}$$

Then

$$\begin{aligned} Z &= A\,(\cos\alpha + j\sin\alpha)\cos\omega t \\ &= A\,\epsilon^{j\alpha}\cos\omega t. \end{aligned} \tag{20}$$

It is clearly seen that the oscilloscope trace is represented in the Z plane by a straight line inclined at an angle α from the positive X axis. The system, therefore, indicates the direction from whence the signal came. The inclusion of frequency conversion in the amplifier is useful to change the value of ω without affecting any other feature of the scheme.

B. Effect of Field Produced by Two Signals

In Fig. 2 is shown the Adcock antenna system in the presence of two waves arriving from arbitrary directions. Wave 1 is given by

$$E_1 = E_m \sin(\omega t + ky') \tag{21}$$

and Wave 2 by

$$E_2 = h\,E_m \sin(\omega t + ky'' + \varphi). \tag{22}$$

Suppose that E_1 is the signal whose bearing is desired and E_2 is an interfering signal such that $0 \leqq h \leqq 1$.

As the electric fields linearly superpose themselves, the differential antenna voltades become

$$e_x = 2e_o r K \cos\alpha \cos\omega t + 2h\,e_o r K \cos(\alpha+\beta)\cos(\omega t+\varphi) \tag{23}$$

$$e_y = 2e_o r K \sin\alpha \cos\omega t + 2h\,e_o r K \sin(\alpha+\beta)\cos(\omega t+\varphi) \tag{24}$$

Again let the signals be amplified and $d_{x\,max}$ be adjusted equal to $d_{y\,max}$. The position of the beam of the oscilloscope is then described by

$$\begin{aligned} Z &= X + jY \\ &= A\,\{\cos\alpha\cos\omega t + h\cos(\alpha+\beta)\cos(\omega t+\varphi) + j[\sin\alpha\cos\omega t + h\sin(\alpha+\beta)\cos(\omega t+\varphi)]\} \\ &= A[\epsilon^{j\alpha}\cos\omega t + h\,\epsilon^{j(\alpha+\beta)}\cos(\omega t+\varphi)]. \end{aligned} \tag{25}$$

Consider now the simplest case, that is, when $\varphi = 0$. Then (25) becomes

$$Z = A(\epsilon^{j\alpha} + h\,\epsilon^{j(\alpha+\beta)})\cos\omega t. \tag{26}$$

The trace is again a straight line but it is inclined at an angle differing from the desired angle α by an error angle θ_e, as shown in Fig. 3. Also from Fig. 3, it is seen that

$$\tan\theta_e = \frac{h\sin\beta}{1 + h\cos\beta}. \tag{27}$$

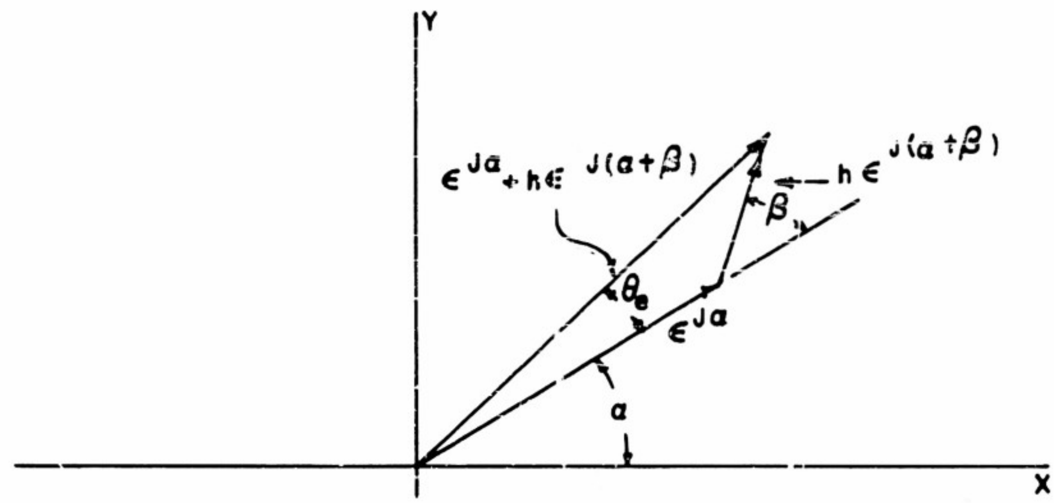

FIGURE 3

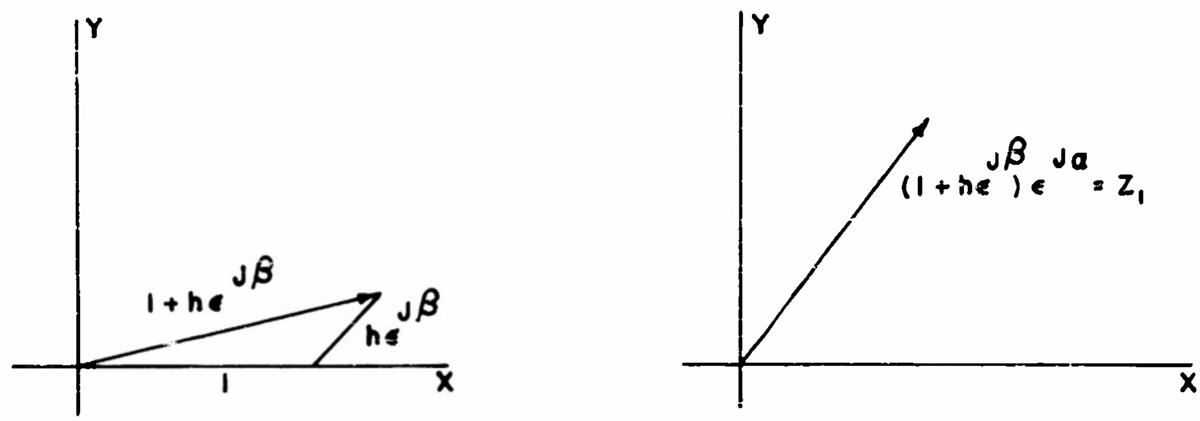

FIGURE 4

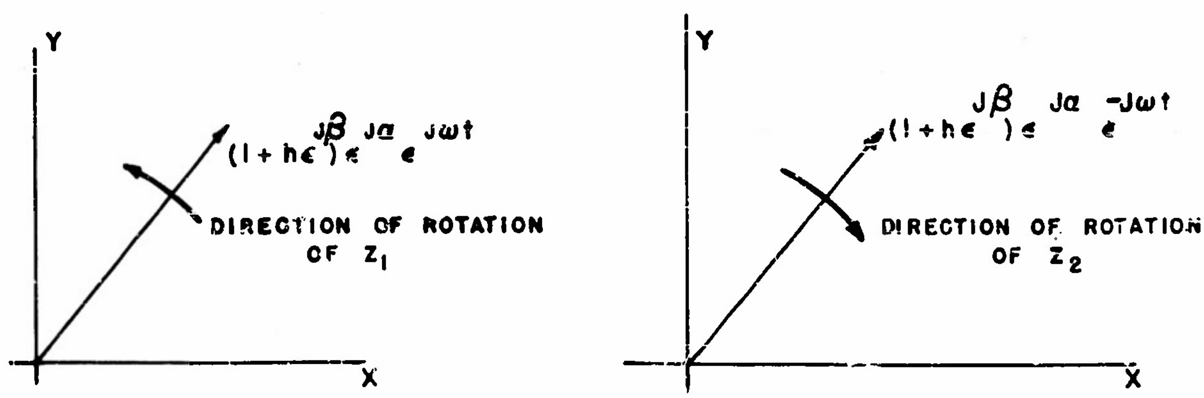

FIGURE 5

In the general case where h, φ, and β do not vanish, the trace described by equation (25) is that of an ellipse. The proof of this is given in Appendix A.

In order to permit easy interpretation of equation (25), it can be rearranged as follows:

$$
\begin{aligned}
Z &= A\,[\epsilon^{j\alpha}\cos\omega t + h\,\epsilon^{j(\alpha+\beta)}\cos(\omega t+\varphi)] \\
&= \frac{A}{2}\,[\epsilon^{j\alpha}(\epsilon^{j\omega t} + \epsilon^{-j\omega t}) + h\,\epsilon^{j(\alpha+\beta)}(\epsilon^{j(\omega t+\varphi)} + \epsilon^{-j(\omega t+\varphi)})] \\
&= \frac{A}{2}\,[(\epsilon^{j\alpha} + h\,\epsilon^{j(\alpha+\beta+\varphi)})\,\epsilon^{j\omega t} + (\epsilon^{j\alpha} + h\,\epsilon^{j(\alpha+\beta-\varphi)})\,\epsilon^{-j\omega t}] \\
&= \frac{A}{2}\,\epsilon^{j\alpha}\,[(1+h\,\epsilon^{j(\beta+\varphi)})\,\epsilon^{j\omega t} + (1+h\,\epsilon^{j(\beta-\varphi)})\,\epsilon^{-j\omega t}] \\
&= Z_1\,\epsilon^{j\omega t} + Z_2\,\epsilon^{-j\omega t} \qquad (28)
\end{aligned}
$$

where

$$Z_1 = \frac{A}{2}\,\epsilon^{j\alpha}\,(1+h\,\epsilon^{j(\beta+\varphi)})$$

$$Z_2 = A\,\epsilon^{j\alpha}\,(1+h\,\epsilon^{j(\beta-\varphi)}).$$

The locus of Z can now be determined in terms of vectors Z_1 and Z_2, each of which are dependent on h, β, and φ, and which rotate in opposite directions at the same constant rate. Figures 4, 5, and 6 show the construction of the Z locus for the case of $\varphi = 0$. In this case, of course, $Z_1 = Z_2$ and the locus of Z is a straight line.

This method of construction to obtain the Z locus is now applied to the case where $\varphi \neq 0$. In this, the general case, the shape is not easily visualized from equation (25) but is readily interpreted by using (28). Figure 7 shows that the effect of $\varphi \neq 0$ on Z_1 and Z_2 is to make $Z_1 \neq Z_2$ in which case the locus of Z becomes elliptic as shown in Fig. 8. The indicated direction of arrival is read as the inclination of the major axis of the ellipse. This indicated bearing is seen to differ from the true bearing α by the error angle θ_ϵ. The derivation of this error angle is presented in Appendix B.

Figures 9 and 10 illustrate the indication resulting from two signals of equal magnitude arriving at angles 25° apart with a time phase difference between the two of 180°. It is seen to be a straight line at right angles to the bisector of the angle between the signals. This is a "worst case" drawn to illustrate the runious effect of certain ranges of φ on the indicator accuracy.

C. The Envelope of the Loci of Z.

It has been shown in the foregoing discussion that for each combination of the parameters α, β, φ, and h, the Z locus is an ellipse or a straight line (degenerate ellipse). Referring to Fig. 11 and considering equation (25)

$$Z = A\,[\epsilon^{j\alpha}\cos\omega t + h\,\epsilon^{j(\alpha+\beta)}\cos(\omega t+\varphi)] \qquad (25)$$

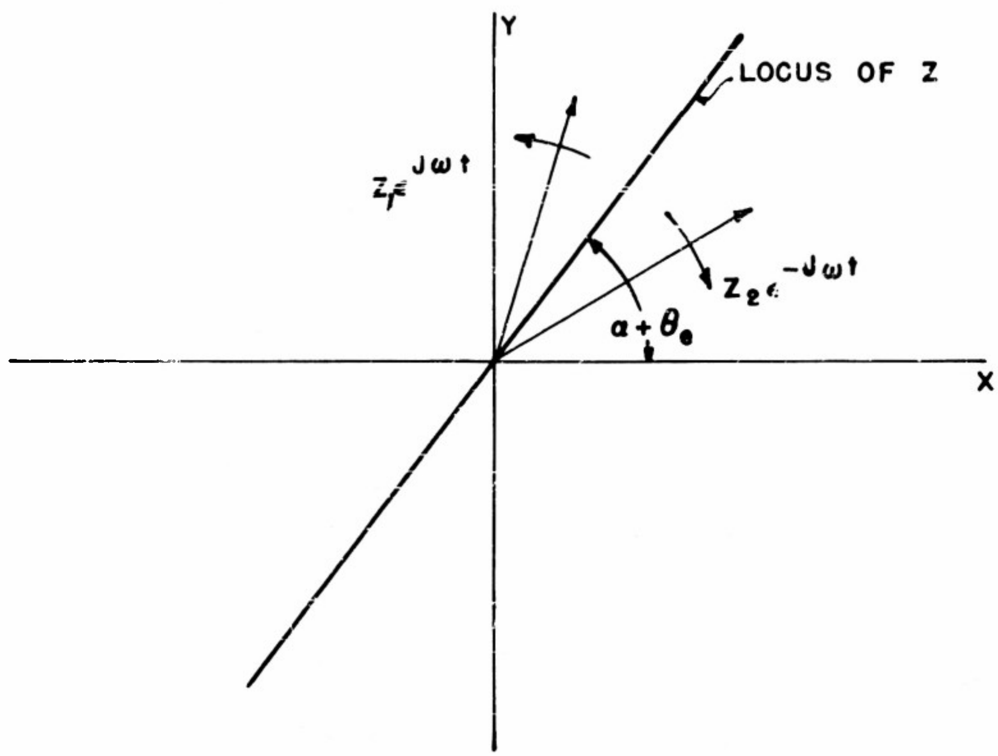

FIGURE 6

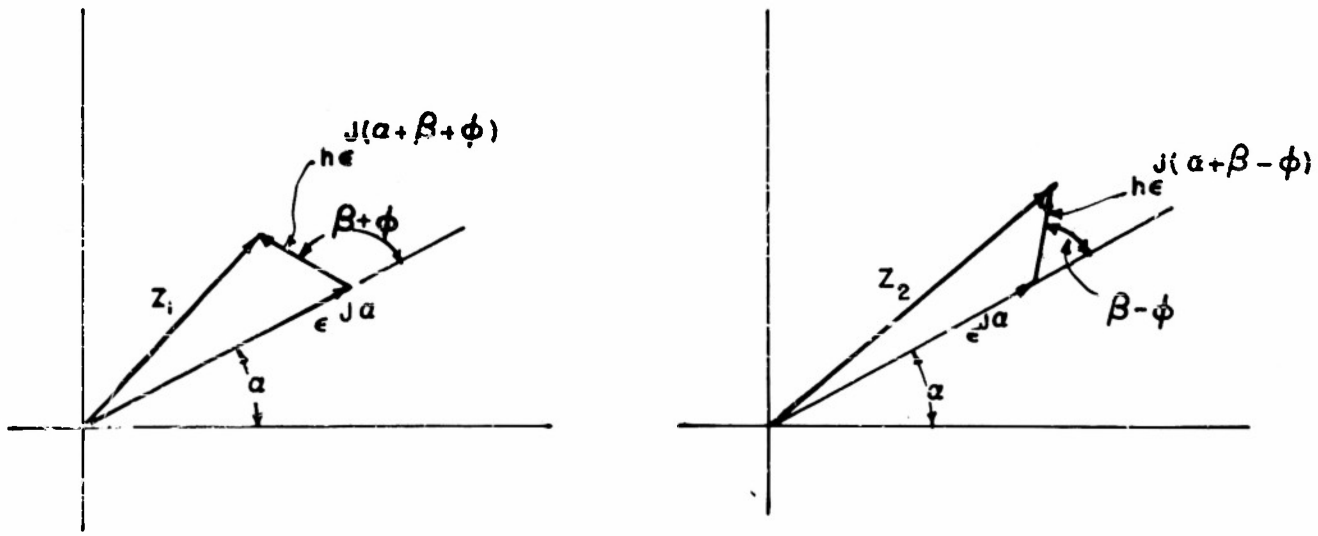

FIGURE 7

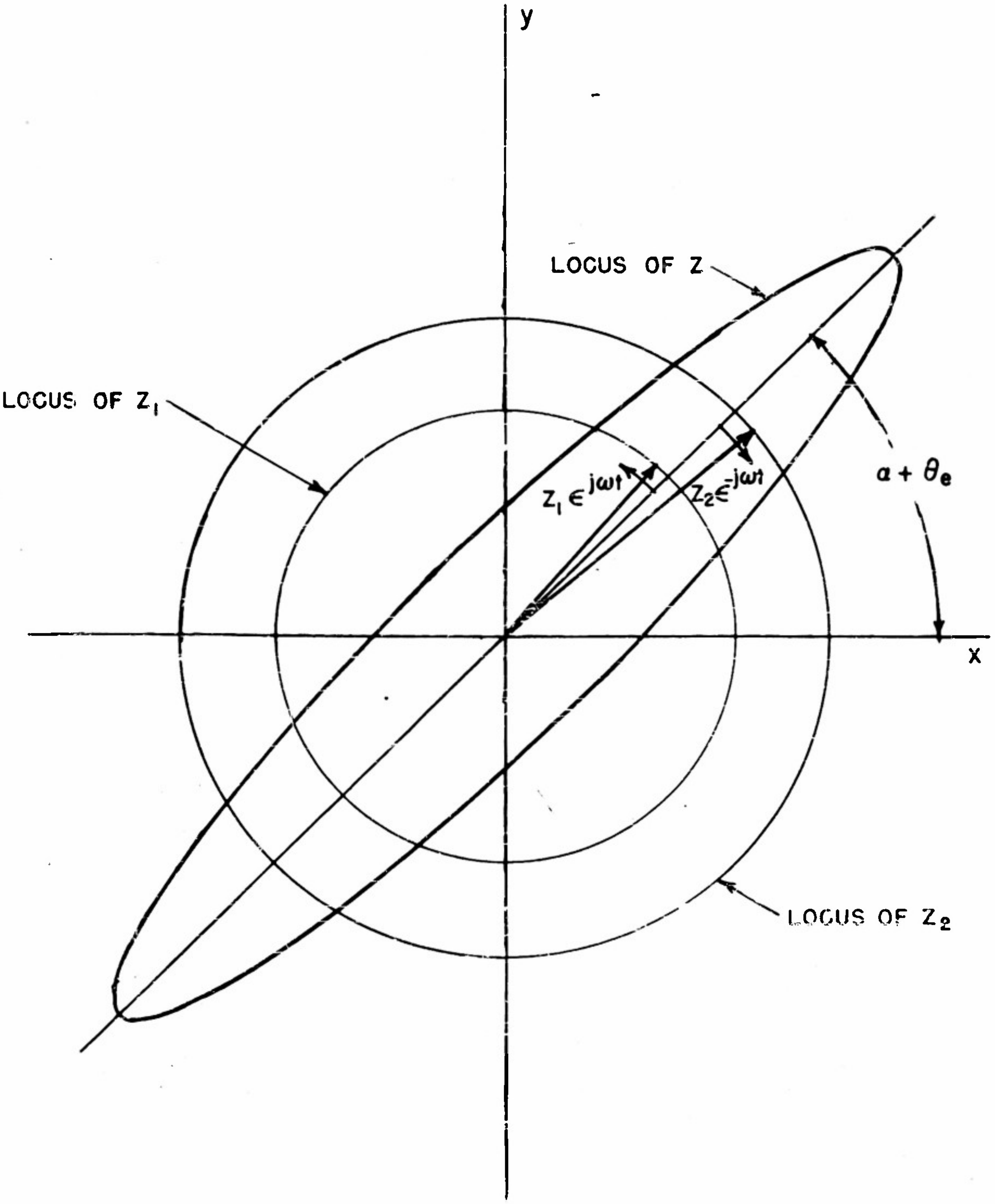
y
LOCUS OF Z
LOCUS OF Z_1
$Z_1\epsilon^{j\omega t}$
$Z_2\epsilon^{-j\omega t}$
$\alpha+\theta_e$
x
LOCUS OF Z_2

FIGURE 8

$h = 1$
$\phi = 180°$
$\beta = 25°$

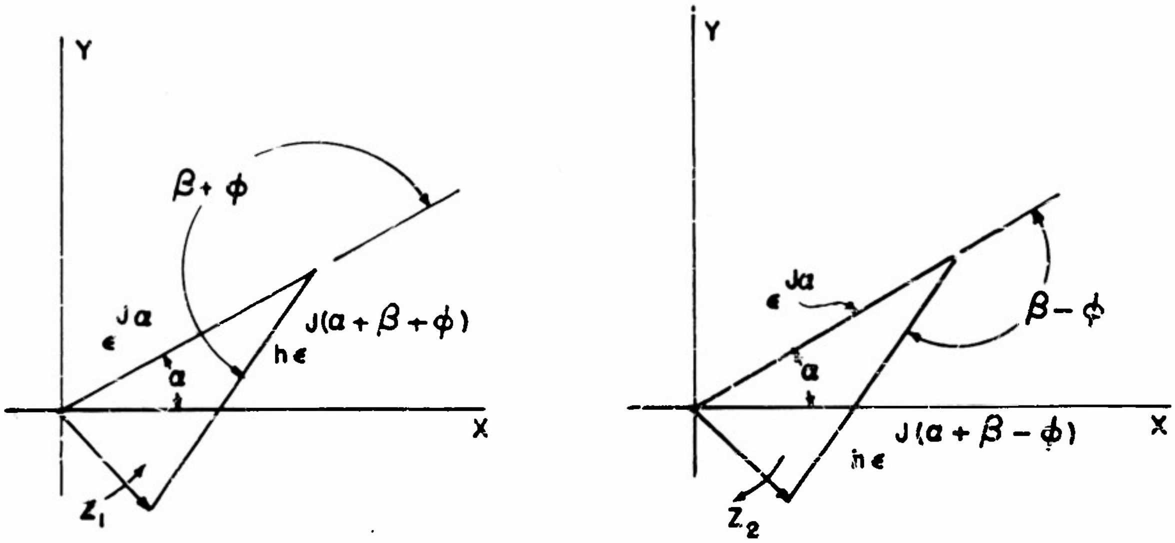

FIGURE 9

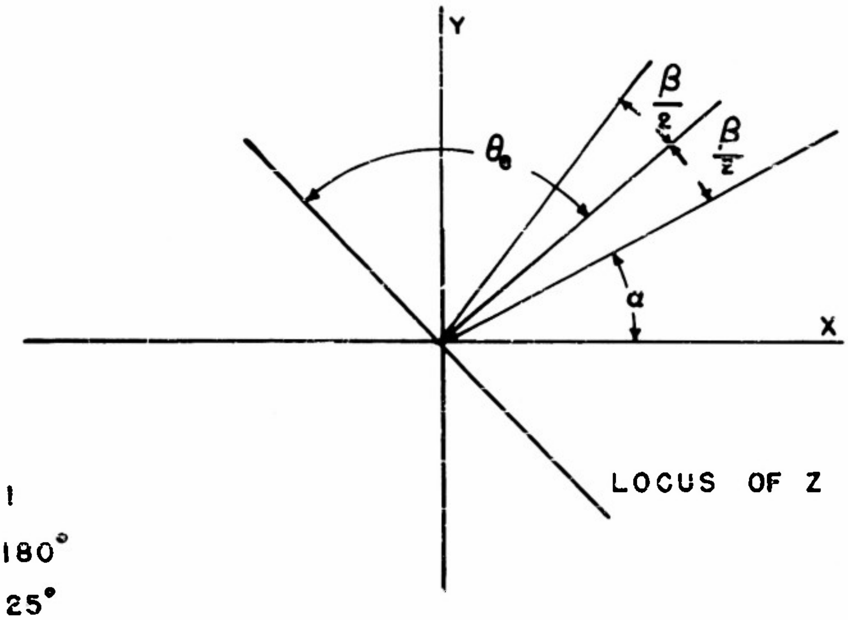

$h = 1$
$\phi = 180°$
$\beta = 25°$

FIGURE 10

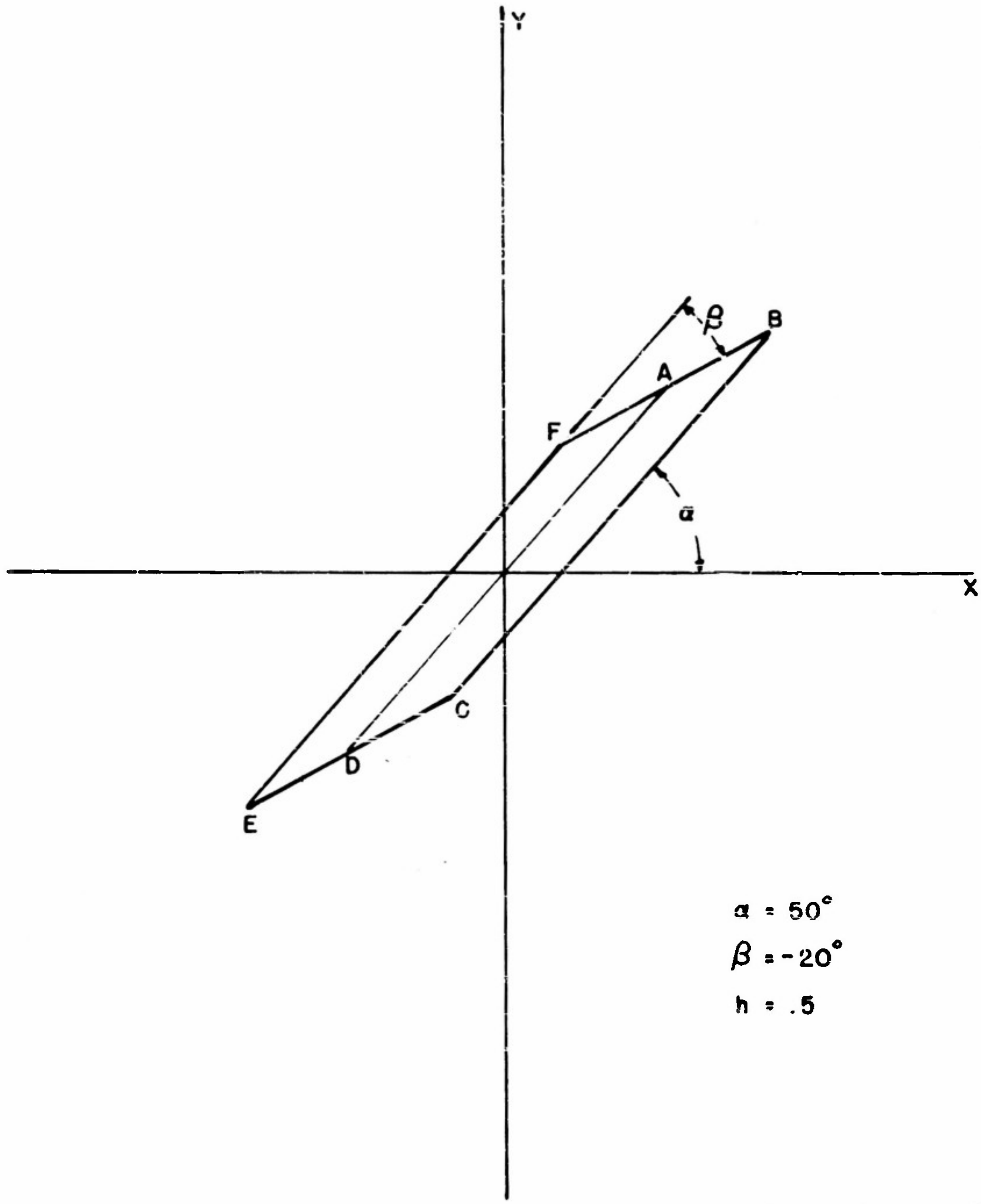

FIGURE II

ENVELOPE OF THE LOCI OF Z

it is possible to determine the possible values of Z in order to establish the shape of the envelope. At a time when $\omega t = 0$, $\varphi = \pi/2$. The first term, $\epsilon^{j\alpha} \cos \omega t$, positions the oscilloscope beam at the point A, and the second term, $\epsilon^{j(\alpha+\beta)} \cos (\omega t+\varphi)$ has no effect. Let φ vary toward zero. The variation of the second term moves Z over to point B. Now let ωt increase positively and φ vary toward negative values so that $\epsilon^{j(\alpha+\beta)} \cos (\omega t+\varphi)$ maintains its maximum positive value, then Z traverses the line BC. At C, $\omega t = \pi$ and $\varphi = -\pi$. By letting φ vary toward zero and holding ωt constant, Z traverses the line CE. At E, $\omega t = \pi$ and $\varphi = \pi$. Let ωt increase positively and φ vary so that $\epsilon^{j(\alpha+\beta)} \cos (\omega t+\varphi)$ maintains its maximum negative value, then Z traverses the line EF. At F, $\omega t = 2\pi$ and $\varphi = \pi$. Let φ vary toward zero, holding ωt constant. At $\omega t = 2\pi$, $\varphi = \pi/2$ and Z is again at A. This parallelogram shaped path represents the maximum values that Z can have. The parallel sides EF and CB lie at an angle α equal to the angle of arrival of Wave 1, while the parallel sides EC and FB lie at an angle $\alpha+\beta$ which is the angle of arrival of Wave 2. The ratio of length of the shorter to the longer side is equal to h. For any fixed value of the parameters, α, β, φ, and h, Z varies only as a function of ωt and described an elliptic path lying within and tangent at its extremes to the parallelogram shown.

In Appendix C is presented an extension of the above argument to cases in which more than one interfering signal is present.

V. WIDE APERTURE DISTRIBUTION OF NARROW APERTURE WATSON-WATT SYSTEMS

In section IV it was shown that the envelope of the elliptical oscilloscopic patterns for a single Watson Watt system with two incoming signals present is a parallelogram (when all parameters except the time phase between the two signals remain constant and this time phase parameter varies over all possible values.) The sides of the parallelo gram are parallel to the directions of arrival of the two incoming signals and the lengths of the sides are proportional to the strengths of the two incoming signals. Thus, the directions of arrival can be completely resolved if the time phase parameter can be made to vary.

One promising technique for obtaining variations in the time phase parameter is to distribute a number of identical Watson Watt systems over a region in the interference field which is reasonably large in terms of wavelengths. In a well designed distribution, the time phase difference between the two signals would then vary apprecia bly from system to system, as shown in Appendix C, and these time phase differences should be reasonable evenly space from 0° to 180°. Conse quently, the ellipses indicating the bearing for each system should represent sufficiently divergent inclinations of all possible ellipses resulting from all possible time phase differences. These ellipses could then be optically superimposed, either on the face of a multi beam oscilloscope tube, or on an optical screen, using separate oscilloscope tubes and mirror reflector techniques to give the super position. Figure 12 gives a schematic diagram of such a scheme. If the systems (including the superposition scheme) have all been adjusted to give identical operation, then the envelope resulting from the ellipses of the distributed systems must be exactly the same parallelogram as for a single system with a varying time phase parameter. Furthermore, the envelope is determined instantaneously, assuming that there are enough ellipses sufficiently dispersed over the possible positions.

This technique for resolving the direction of arrival of two interfering signals can be extended to three or more interfering signals. It is shown in Appendix C that for three incoming signals the envelope of the ellipses is a six sided polygon with opposite sides parallel and equal to each other. The pairs of parallel sides are parallel respec tively, to the directions of arrival of the signals they represent, and have lengths proportional to the relative magnitude of these signals. Thus, it is seen that the six sided parallelogram completely resolves the three signals exactly as does the quadrilateral parallelogram for two signals. The theory can be extended to n incoming signals repre sented by a polygonal envelope with 2n sides.

For the case of two signals it is possible to determine by eye the approximate tangents to the family of ellipses, however, for greater accuracy an electronic parallelogram-cursor is described which would not only trace the actual envelope but also permit it to be adjusted tangent to the ellipses for two incoming signals. Plate (1) contains photo graphs illustrating the seven ellipses that result from a particular (typical) condition of two interfering signals at each of a series of seven Watson Watt direction finders evenly spaced about the periphery of a circle 5 wavelengths in diameter. The relative magnitude between the

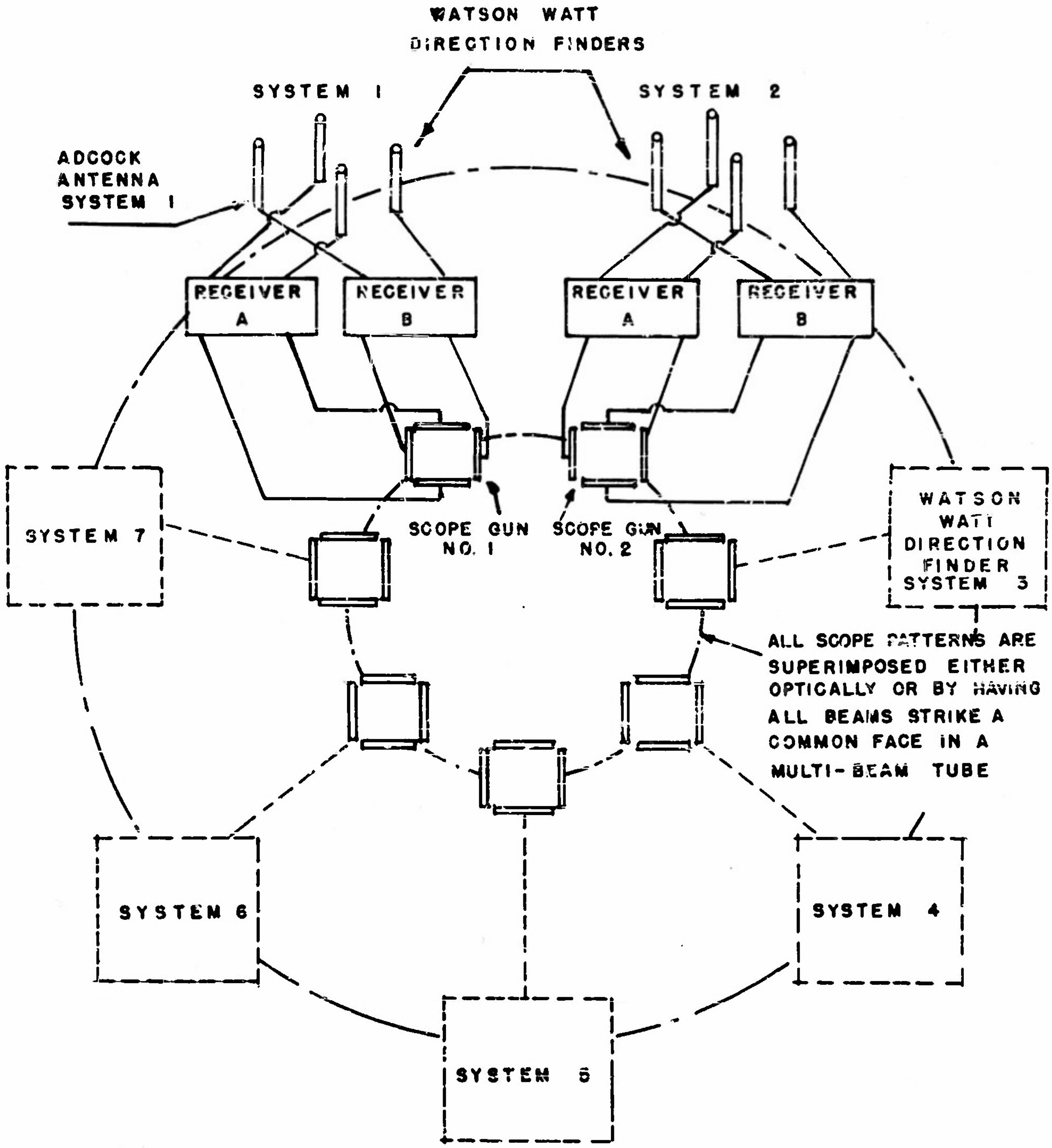

FIGURE 12

WIDE APERTURE DISTRIBUTION OF NARROW-APERTURE WATSON WATT SYSTEMS

PHOTO 1

PHOTO 2

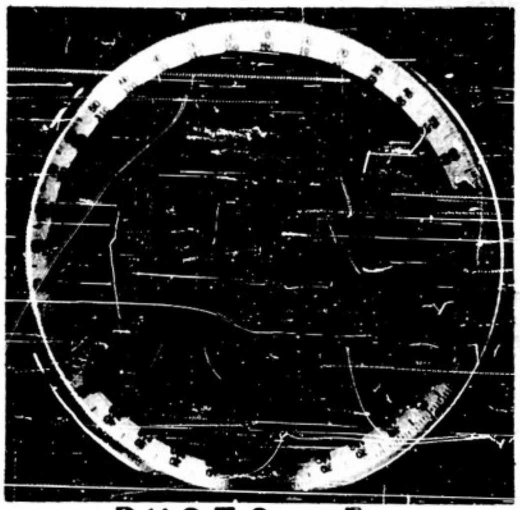

PHOTO 3

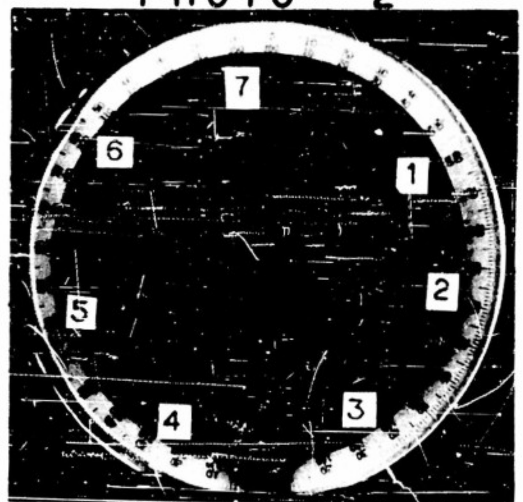

PHOTO 4

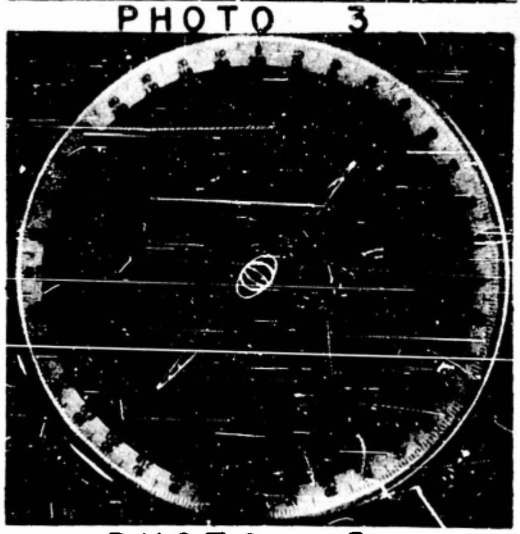

PHOTO 5

PHOTO 6

INDIVIDUAL AND SUPERIMPOSED BEARINGS
FOR A WADONAS OF 7 WATSON-WATT SYSTEMS
EQUALLY SPACED ON A CIRCLE OF 5 λ

$B = 35°$ $B = 45°$ $h = 1°$ $\phi = 355°$

two signals is unity, the bearings of the signals are 45° and 35°, and the time phase difference between the signals at the center of the composite system is 37.5°. Photo 1 illustrates the seven equally spaced systems. Photo 4 illustrates how the ellipses corresponding to each system would appear before super-position. Note that at some locations in the interference field, such as at the location of the systems 1, 2, and 3 time phase difference is nearly 180°. The electromagnetic field is nearly canceled, and the antenna pickup and magnitude of bearing indication are extremely small. Even if the indicated bearing (major axis of the ellipse) can be determined, it is apt to be badly in error. There is no means of insuring that such a situation cannot occur under normal sky-wave propagation conditions if only one Watson-Watt system is utilized.

Photo 5 illustrates how these same ellipses would appear if superimposed, and Photo 6 shows the parallelogram envelope drawn tangent to the ellipses by the electronic cursor. Note that the sides of the parallelogram are at angles 45° and 35°. Photo 2 shows that in the case of only one signal (arriving at 35°), the ellipses of all seven systems become straight lines pointing in the direction of arrival of this signal. Photo 3 shows the case of only the other signal arriving at 45°.

If it is equally probable that a signal arrive from any direction, then a circular distribution of symmetrically disposed unit systems would probably give the best average operation. If, however, the majority of the signals were expected to arrive from a particular sector, then some other distribution such as a linear or semicircular distribution would give optimum performance; i.e., it would assure a maximum number of ellipses of widely varied inclinations for the number of unit systems employed.

From the photo it appears that, in the case of two arriving signals at least, the ellipses from seven systems equally distributed about a circular periphery are adequate to determine the parallelogram shaped envelope. Section VII contains a set of photos illustrating these superimposed ellipses with and without parallelogram shaped envelopes, generated electronically, for what is felt to be typical values of the various parameters. All photos represent seven systems evenly spaced on circles ranging from one to ten wavelengths in diameter.

VI. SIMULATION OF WADONAS OF WATSON-WATTS WITH THE RDF ANALYZER AND EIGHT-BEAM OSCILLOSCOPE

Fourteen channels (see Fig. 13) of the RDF analyzer were used to secure the x and y oscilloscope plate deflection voltages needed for seven beams of the eight-beam oscilloscope. Each element supplied the difference voltage corresponding to that which a differentially connected Adcock antenna pair would produce (see Fig. 14). The eighth beam of the oscilloscope was connected to an electronic cursor, which produces a parallelogram whose sides are adjustable both in length and inclination. In use, the cursor parallelogram is superposed upon the collection of seven ellipses given by the system and its size and shape is adjusted so that the ellipses are enclosed within and tangent to it. The angles of arrival and relative magnitudes of the two signals present are then easily resolved either from the cursor dials or from the oscilloscope scale. A schematic of the cursor circuit is given in Fig. 15. From it one sees that

$$e_x \propto E \cos \alpha \sin \omega t + h E \cos(\alpha+\beta)\sin(\omega+\Delta\omega)t \qquad (29)$$

$$e_y \propto E \sin \alpha \sin \omega t + h E \sin(\alpha+\beta)\sin(\omega+\Delta\omega)t \qquad (30)$$

where α and $\alpha+\beta$ are the rotation angles of synchros No. 1 and No. 2, respectively, from their reference axes. $\Delta\omega$ is a small deviation from ω. e_x and e_y from the cursor are supplied to the amplifier of beam 8 of the oscilloscope. Adjustment of the potentiometers and the synchros allows the parallelogram to be adjusted so that it will fit over the ellipses.

The phase differences of the arrays simulated were calculated for the different cases presented and set up on the 14 channels of the analyzer used for ellipse presentation.

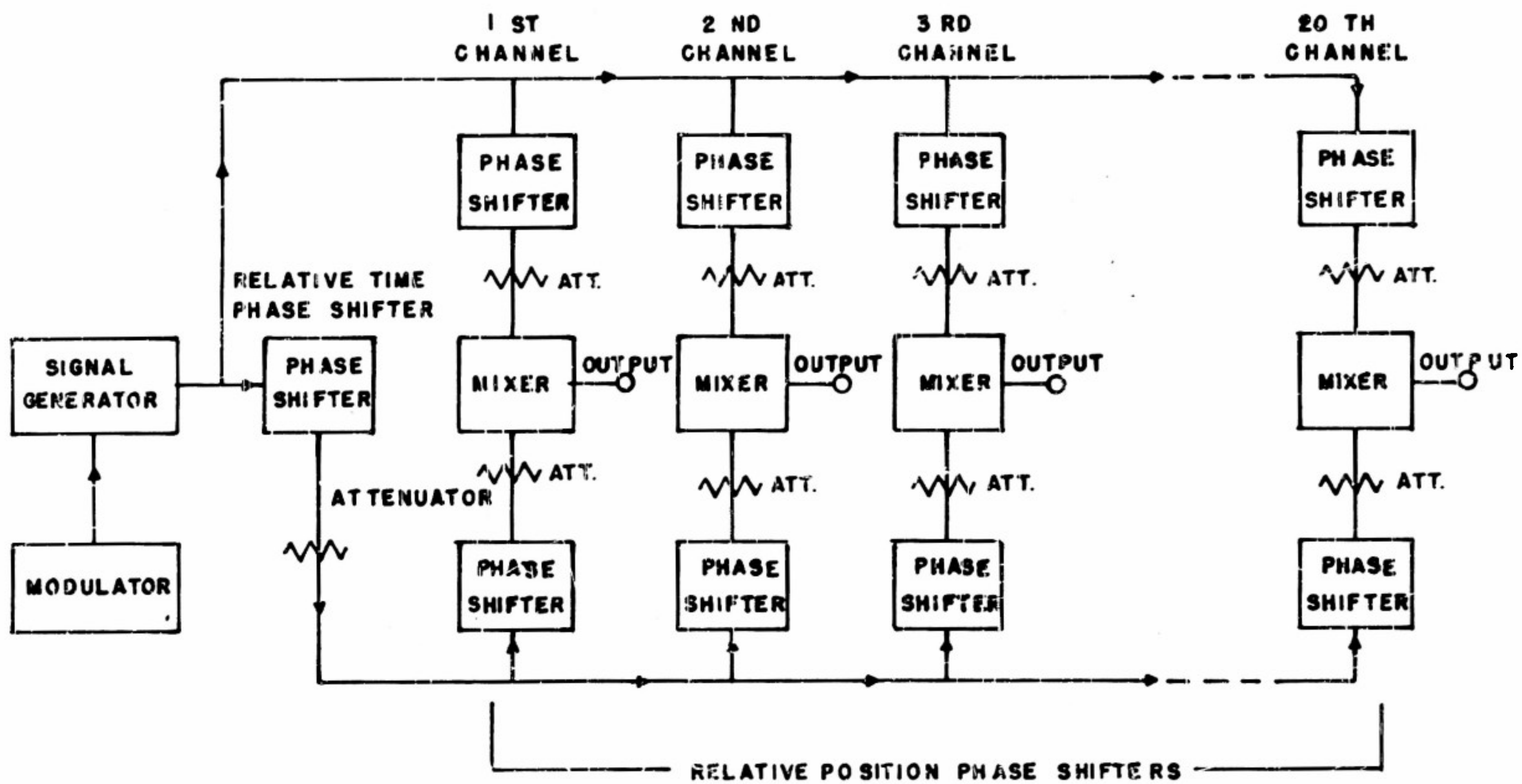

FIGURE 13

BLOCK DIAGRAM OF RDF ANALYZER

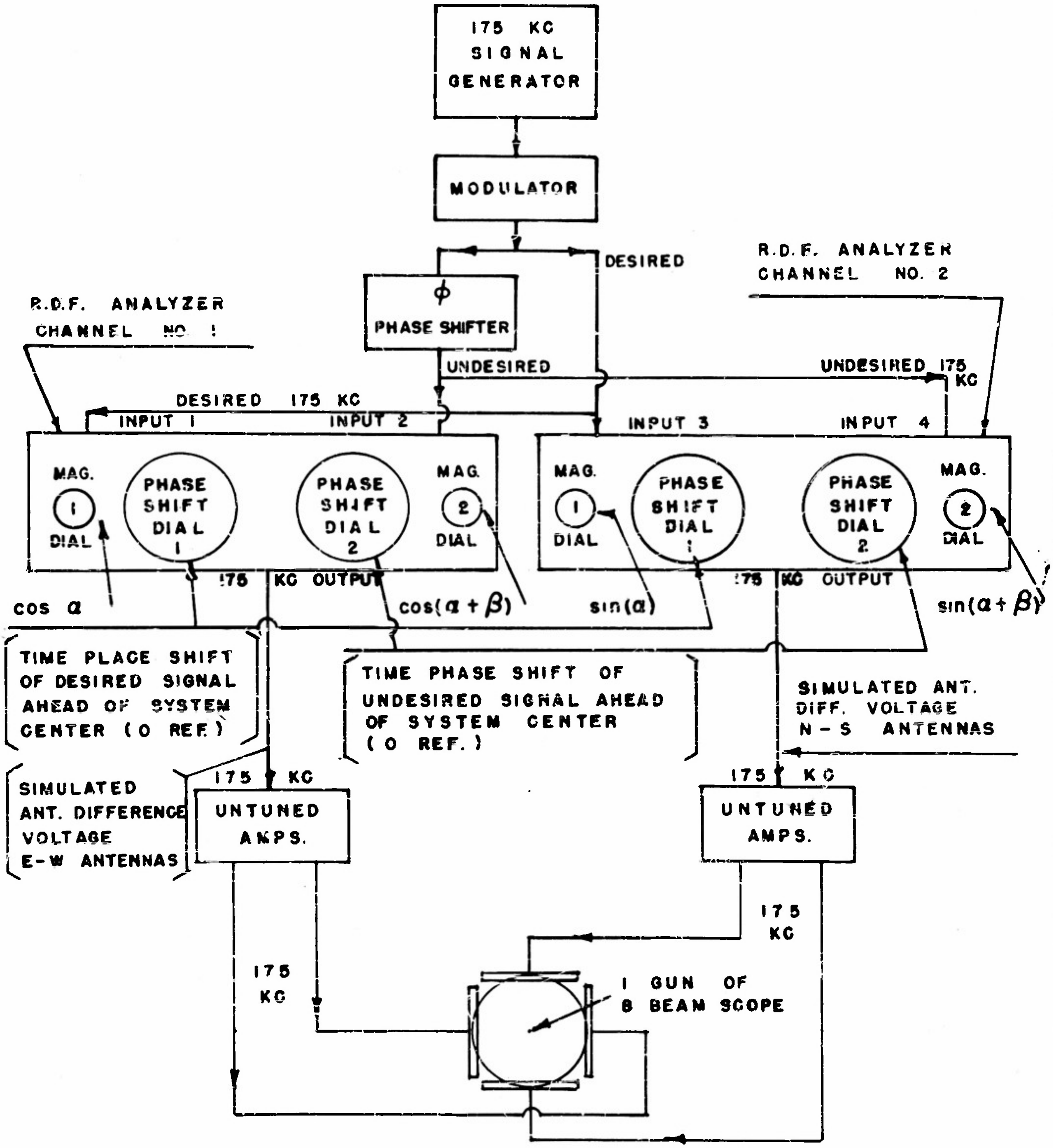

FIGURE 14

TECHNIQUE OF SETTING TWO RDF ANALYZER CHANNELS TO SIMULATE A SINGLE WATSON WATT SYSTEM

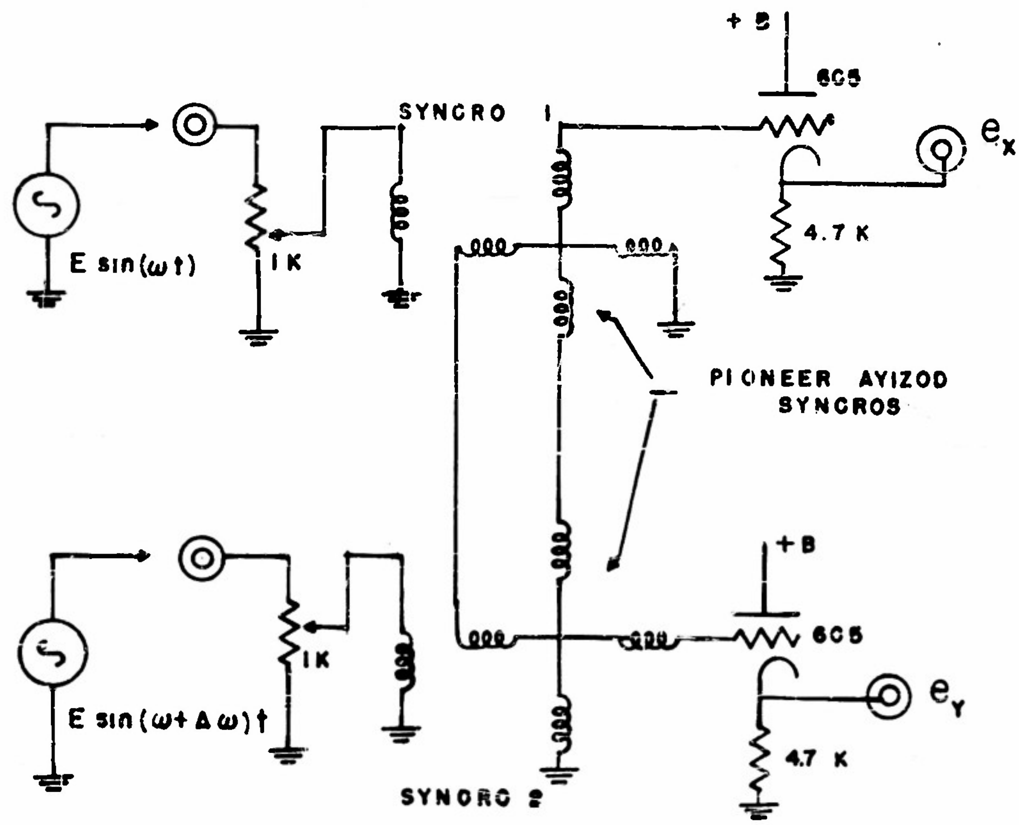

FIGURE 15

SCHEMATIC OF ELECTRONIC CURSOR

VII. CATHODE-RAY INDICATOR PHOTOGRAPHS FOR A SIMULATED WADONAS

Plate I illustrates the make-up of a WADONAS indicator and is described in Section V.

Plates II through V consist of bearing indications with the some range of time phase values, φ, for two signals having a relative magnitude of unity and a separation of 5°. Since each plate is for a different aperture, this series shows the variation in indications as a function of D, the system aperture.

The series of Plates VI through VIII, IX through XI, and XII through XIV consist of photos for a system of $D = 5\lambda$ (considered a useful medium aperture).

Plates VI through VIII show indications for the same range of values for $h = 0.3$, 0.7, and 1. The two arriving signals are separated by 5°.

Plates IX through XI are similar to Plates VI through VIII, but, the two arriving signals are separated by 10°.

Plates XII through XIV are similar to plates VI through VIII, but the two arriving signals are separated by 25°.

Plate XV shows the same set of conditions used in Plates II through V but in this case the relative time phase, φ, is made to vary continously through all possible values. Each photo is for a different aperture, as labeled.

Plate XVI shows the use of an electronic cursor as an aid in the resolution of the parallelogram-shaped envelope produced by two arriving signals. The cursor is of greatest use when the number of unit systems employed is small.

Plate XVII is a photograph of the RDF analyzer, together with the eight-beam oscilloscope used in the WADONAS simulation.

Figure 16 is a diagrammatic sketch based on Plate XVII designating the components of the analyzer.

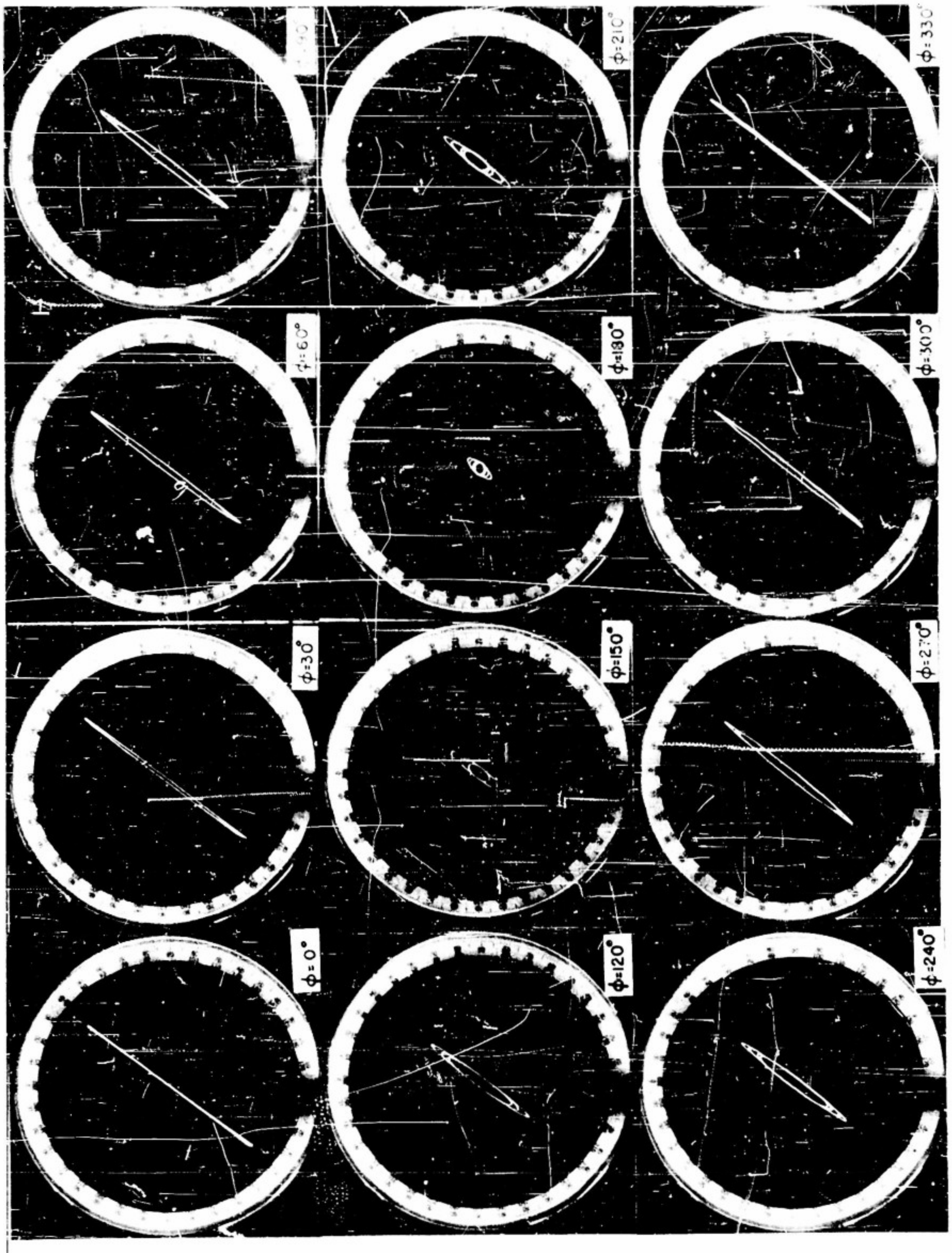

B_1=35° B_2=40° h=1.0 D=λ φ as indicated

COMPOSITE BEARING INDICATION OF A 7—UNIT WADONAS

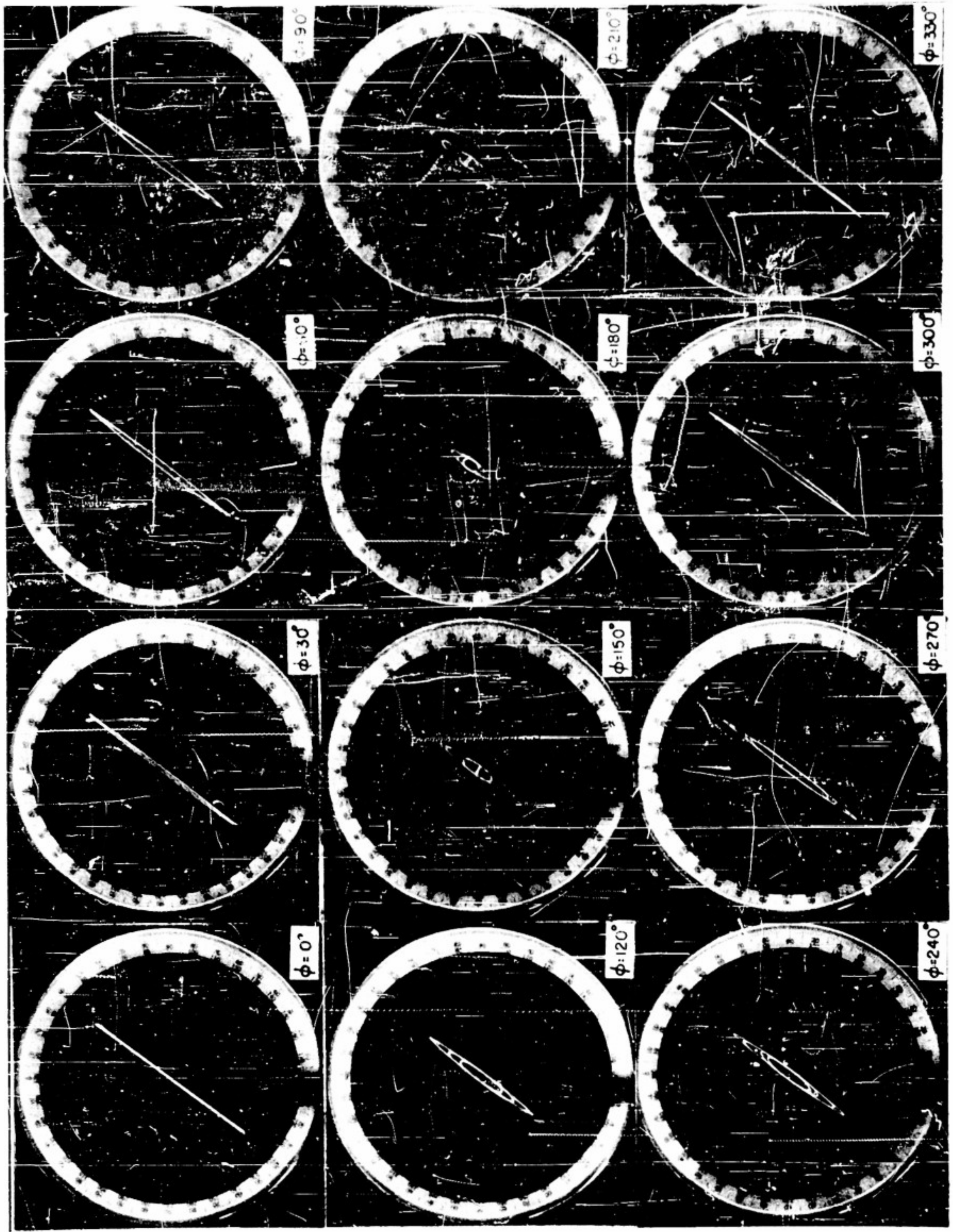

$B_1=35°$ $B_2=40°$ $h=1.0$ $D=2\lambda$ ϕ as indicated

COMPOSITE BEARING INDICATION OF A 7-UNIT WADONAS

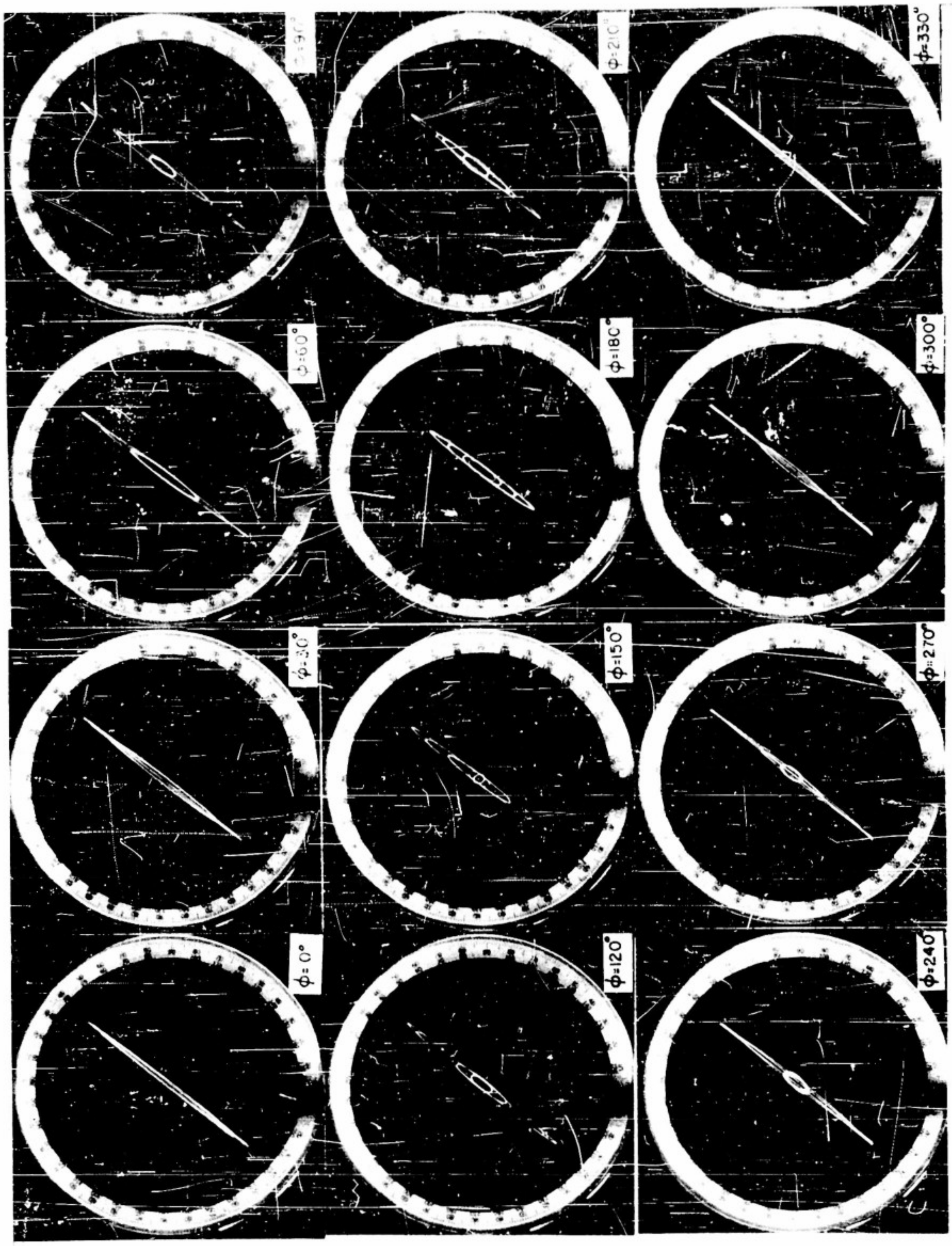

$B_1=35°$ $B_2=40°$ $h=1.0$ $D=5\lambda$ ϕ as indicated

COMPOSITE BEARING INDICATIONS OF A 7-UNIT WADDLAS

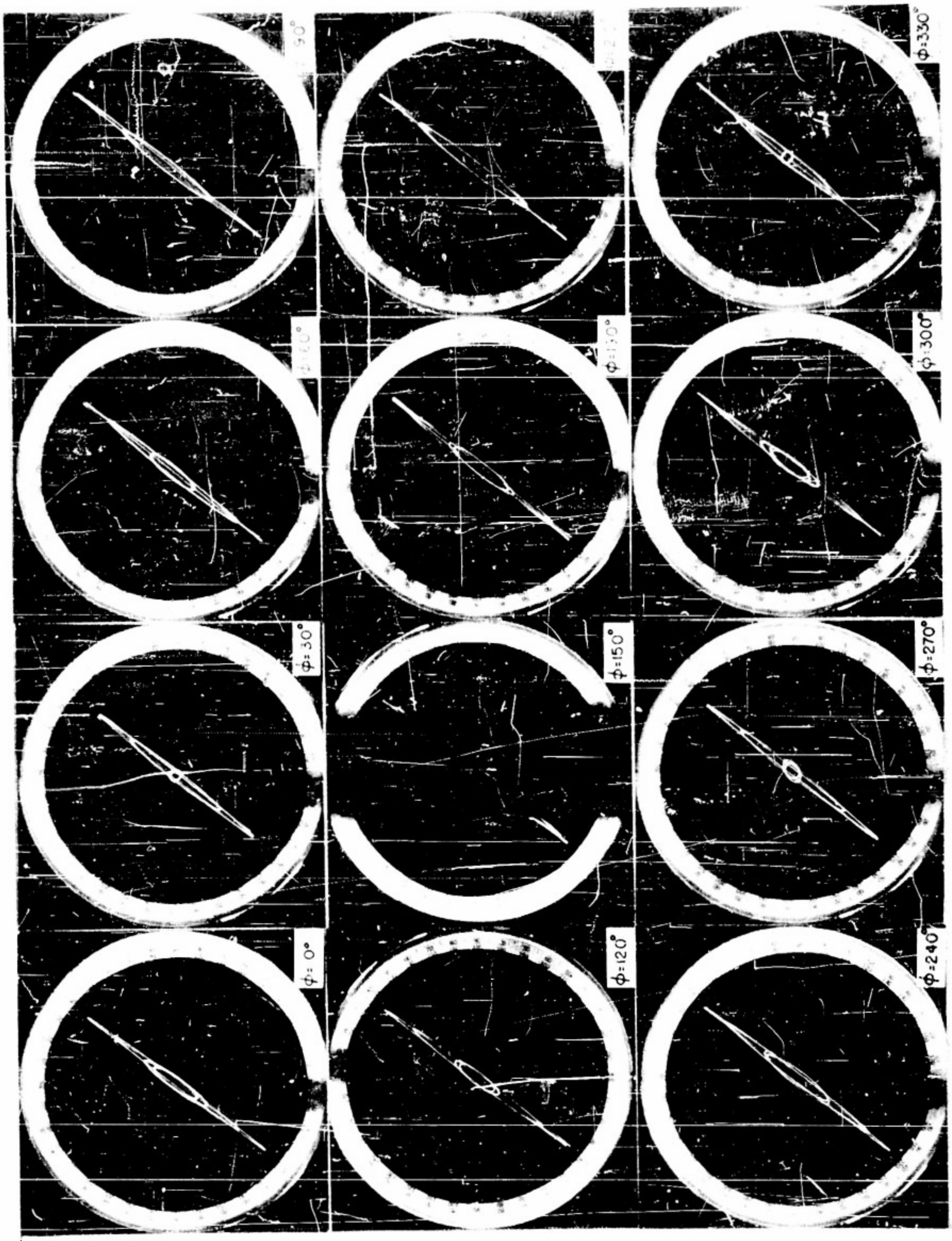

$B_1=35°$ $B_2=40°$ h=1.0 D=10λ φ as indicated

COMPOSITE BEARING INDICATION OF A 7-UNIT WADONAS

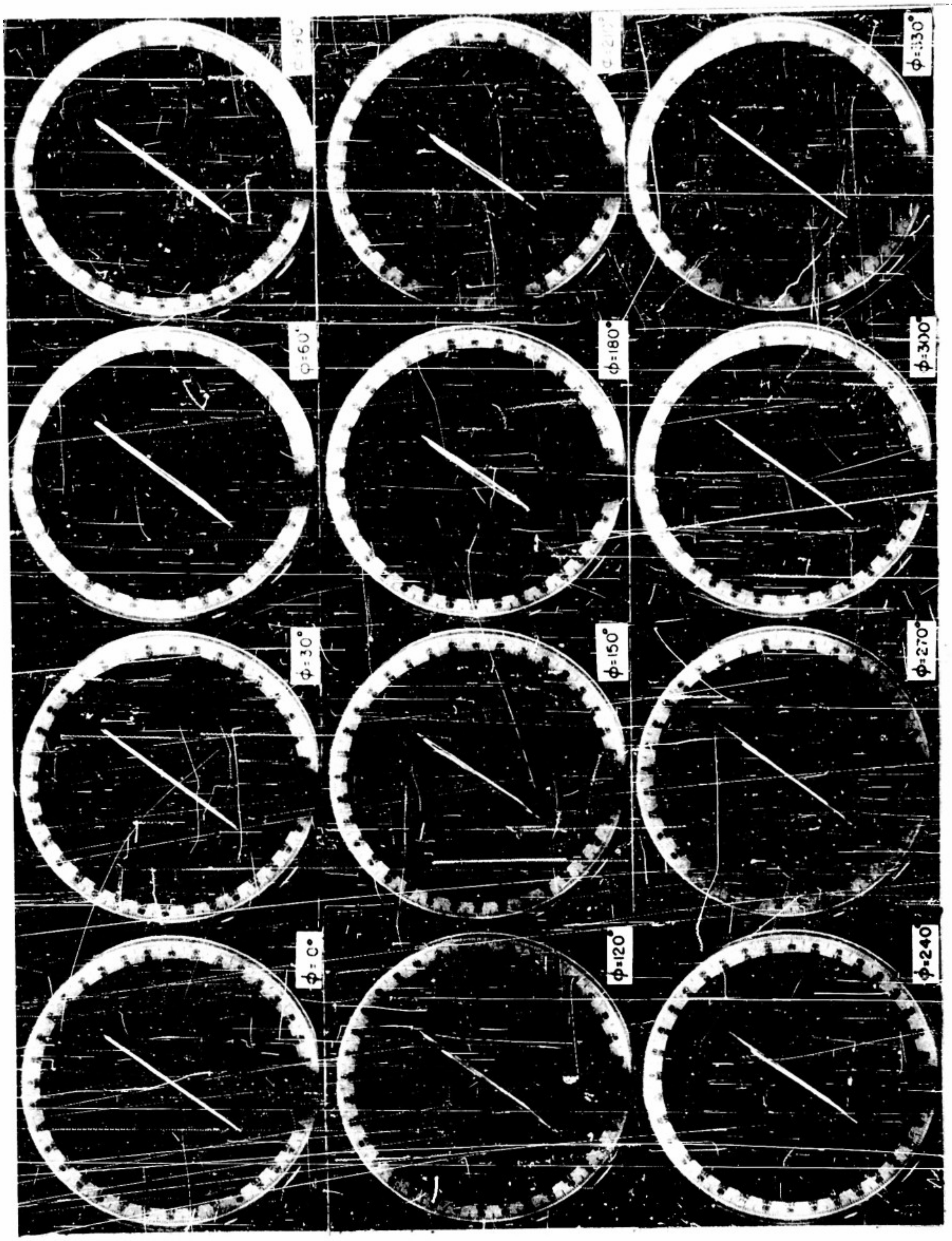

$B_1=35°$ $B_2=40°$ $h=0.3$ $D=5\lambda$ ϕ as indicated

COMPOSITE BEARING INDICATION OF A 7-UNIT WADONAS

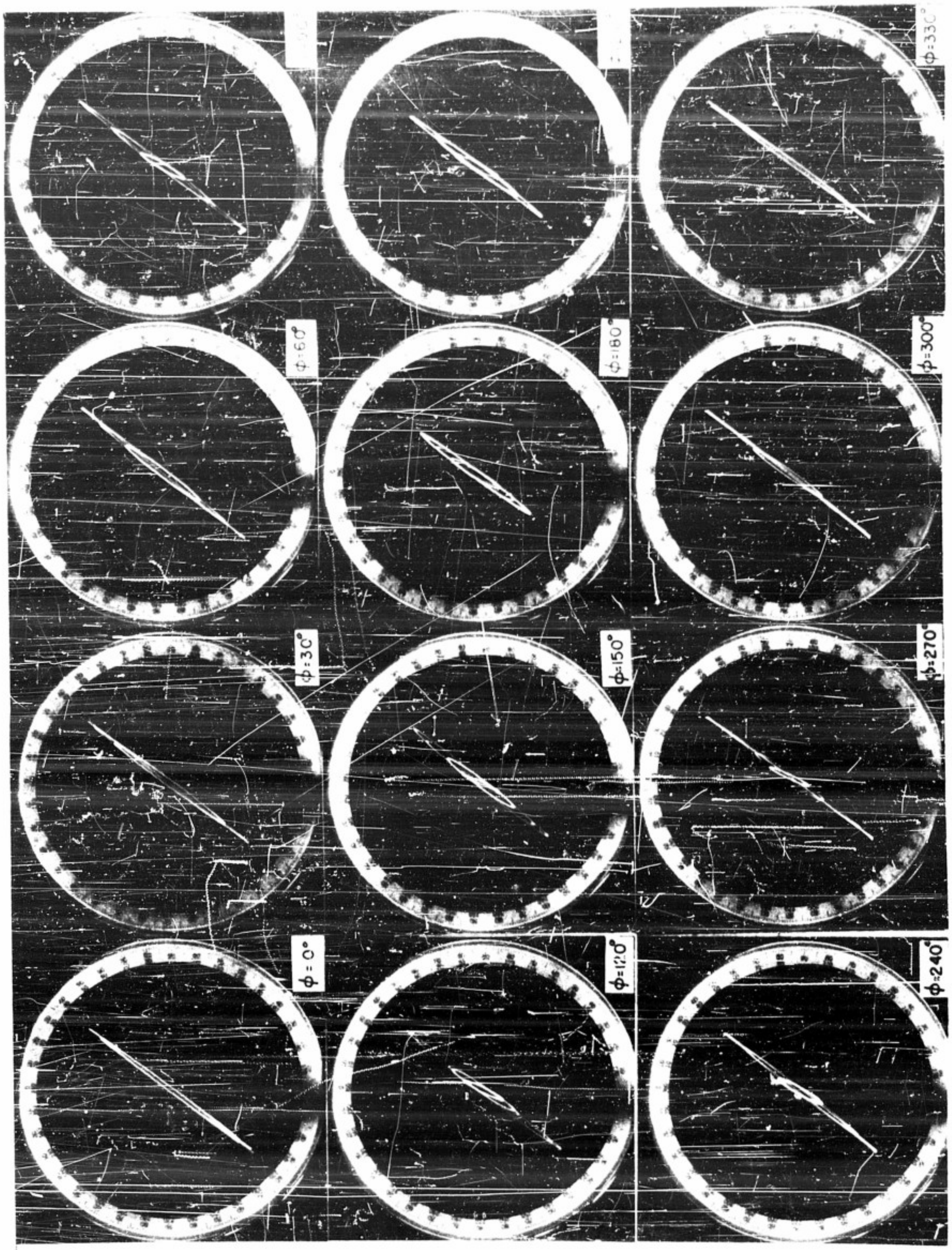

$B_1=35°$ $B_2=40°$ $h=0.7$ $D=5\lambda$ ϕ as indicated

COMPOSITE BEARING INDICATION OF A 7-UNIT WADONAS

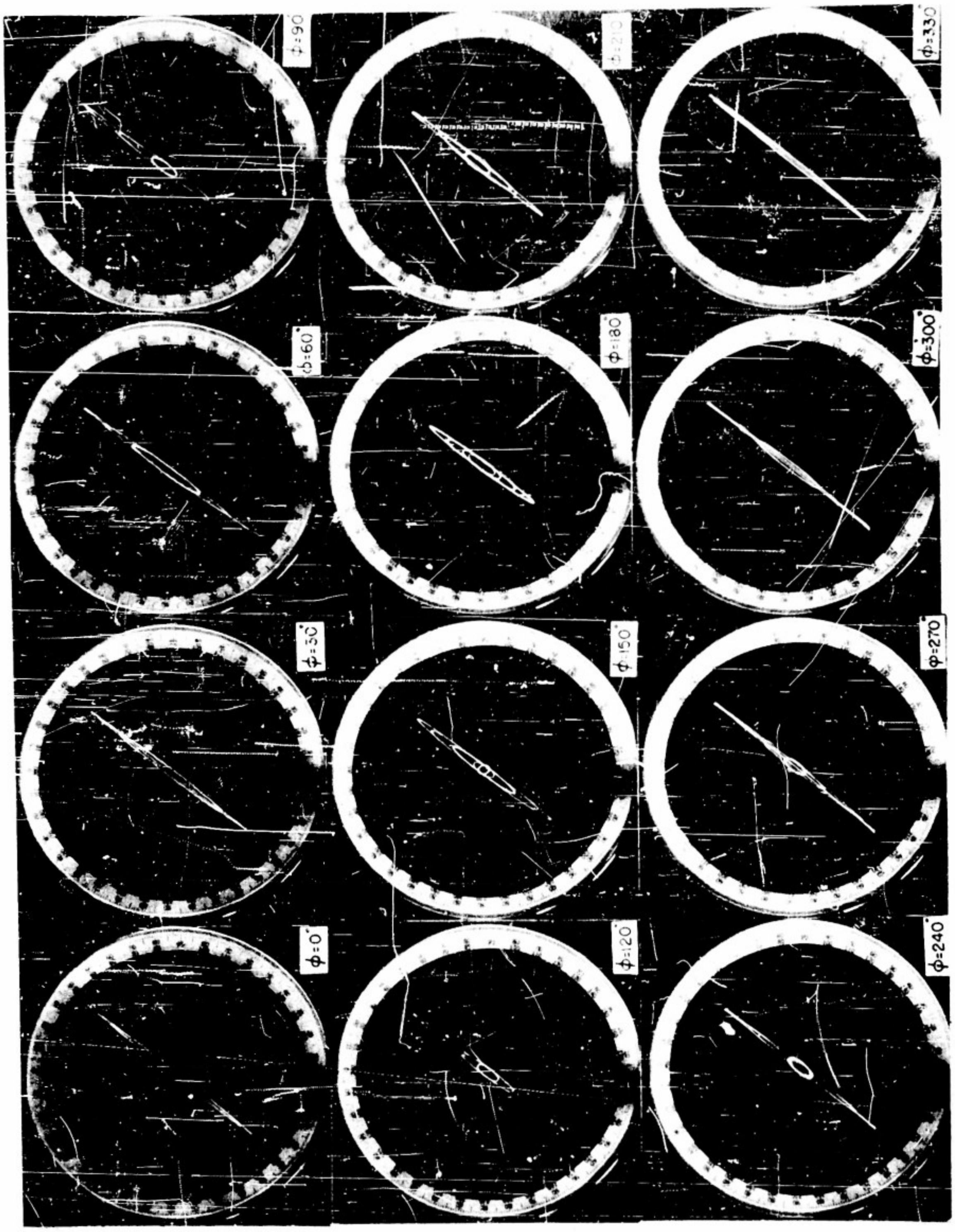

$B_1=35^\circ$ $B_2=40^\circ$ $h=1.0$ $D=5\lambda$ ϕ as indicated

COMPOSITE BEARING INDICATION OF A 7-UNIT WADONAS

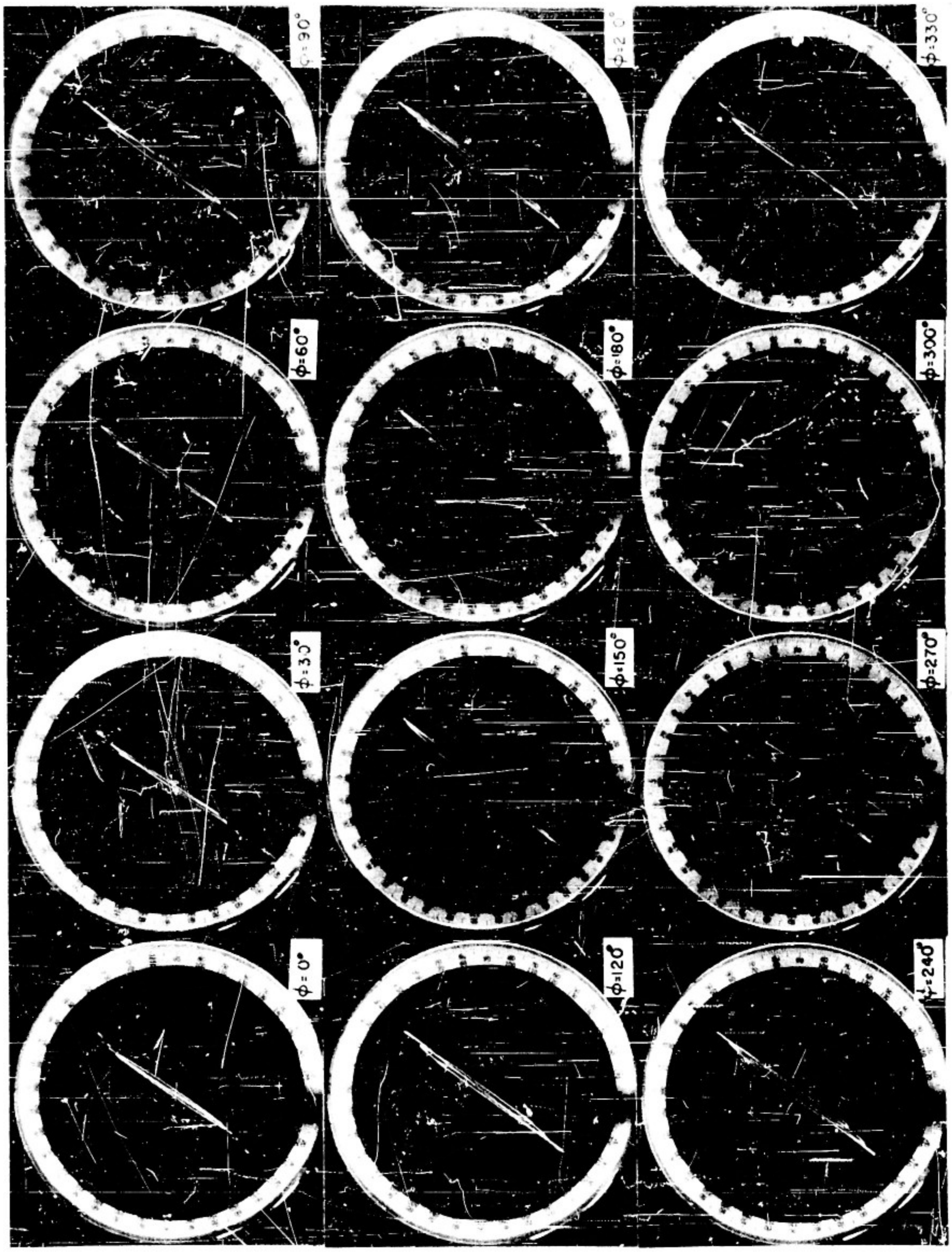

B_1=35° B_2=45° h=0.3 D=5λ ϕ as indicated

COMPOSITE BEARING INDICATION OF A 7-UNIT WADONAS

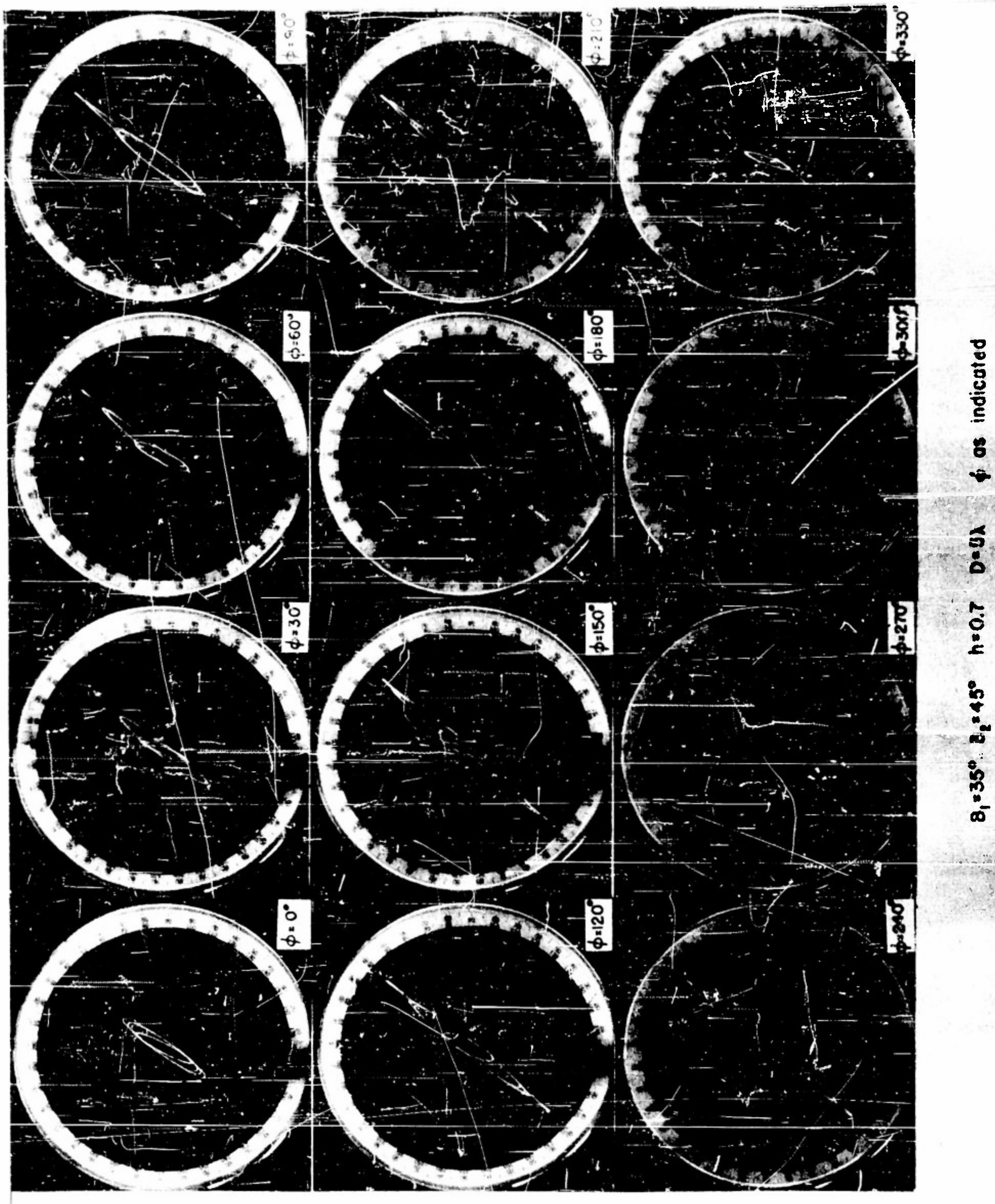

COMPOSITE BEARING INDICATION OF A 7–UNIT WADONAS

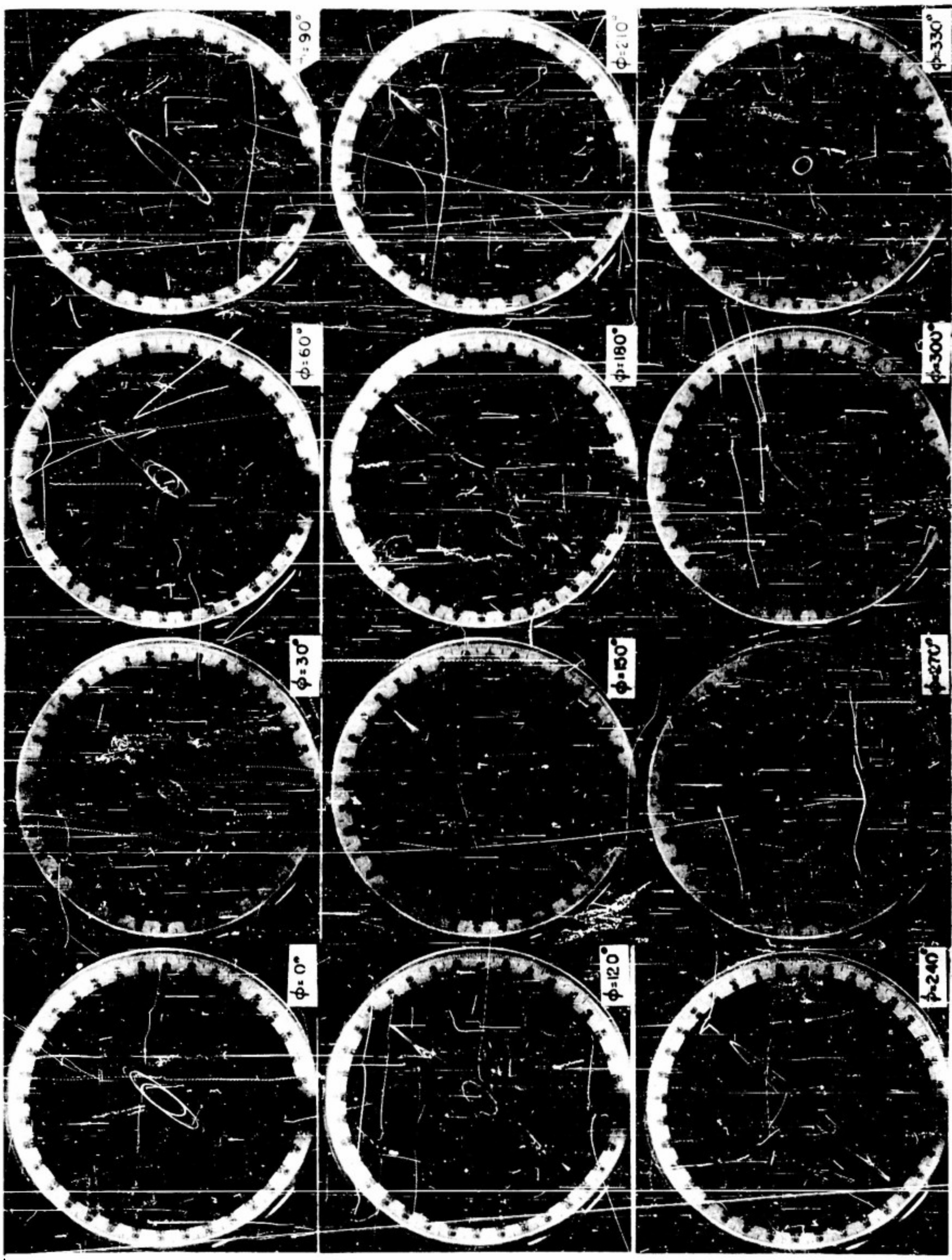

$B_1 = 35°$ $B_2 = 45°$ $h = 1.0$ $D = 5\lambda$ ϕ as indicated

COMPOSITE BEARING INDICATION OF A 7—UNIT WADONAS

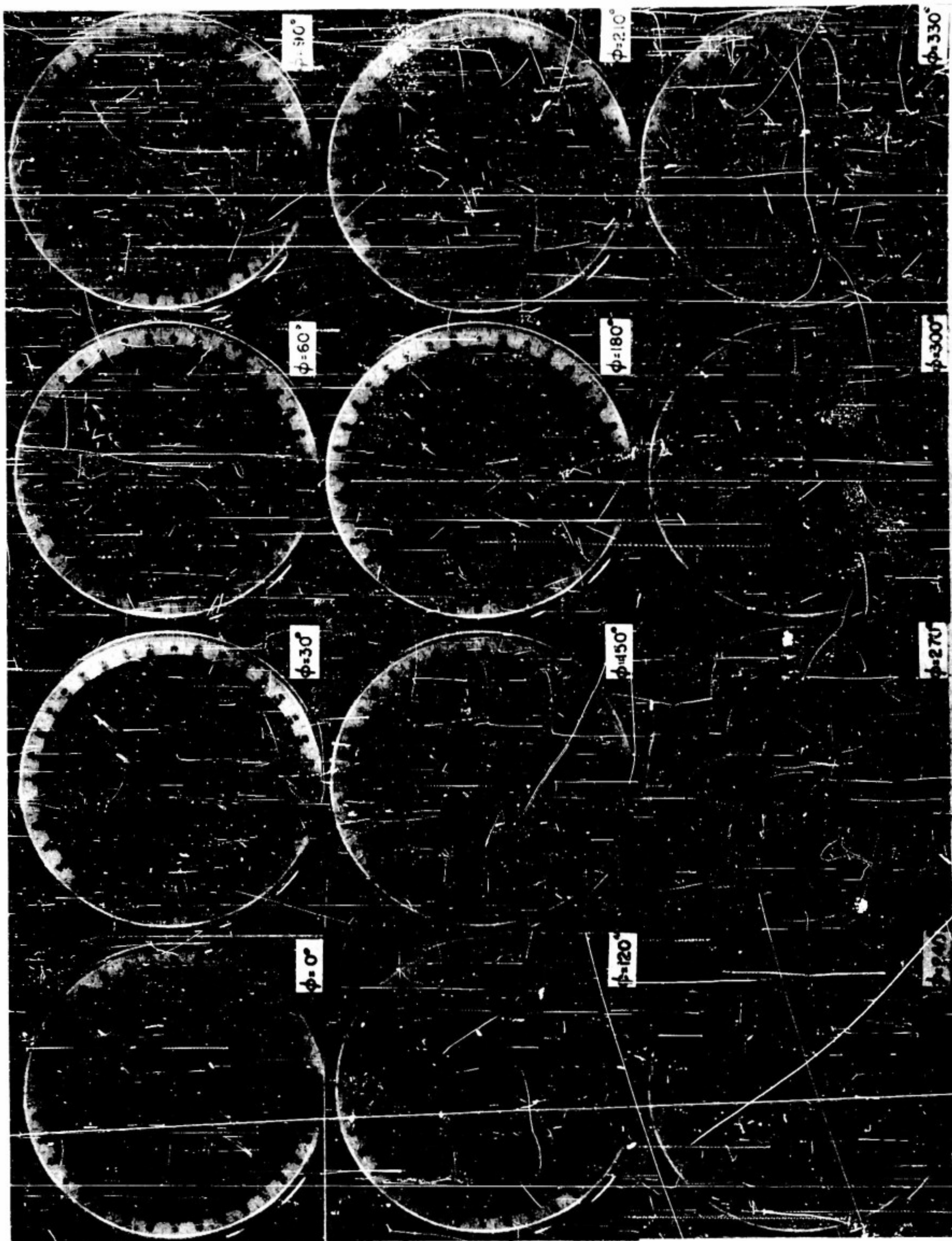

$B_1=35°$ $B_2=60°$ $h=0.3$ $D=5\lambda$ ϕ as indicated

COMPOSITE BEARING INDICATION OF A 7-UNIT WADONAS

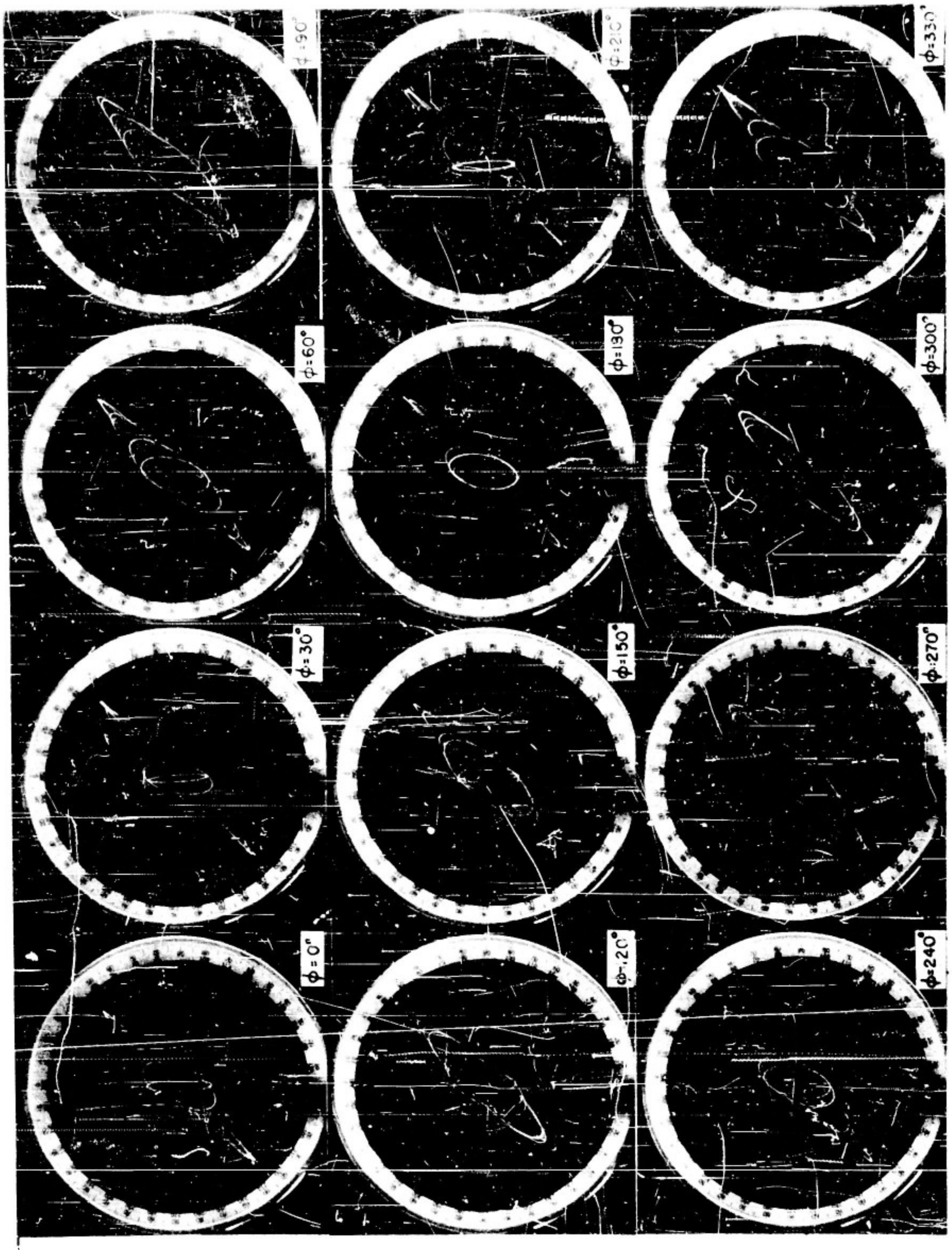

$B_1=35°$ $B_2=60°$ $h=0.7$ $D=5\lambda$ ϕ as indicated

COMPOSITE BEARING INDICATION OF A 7—UNIT WADONAS

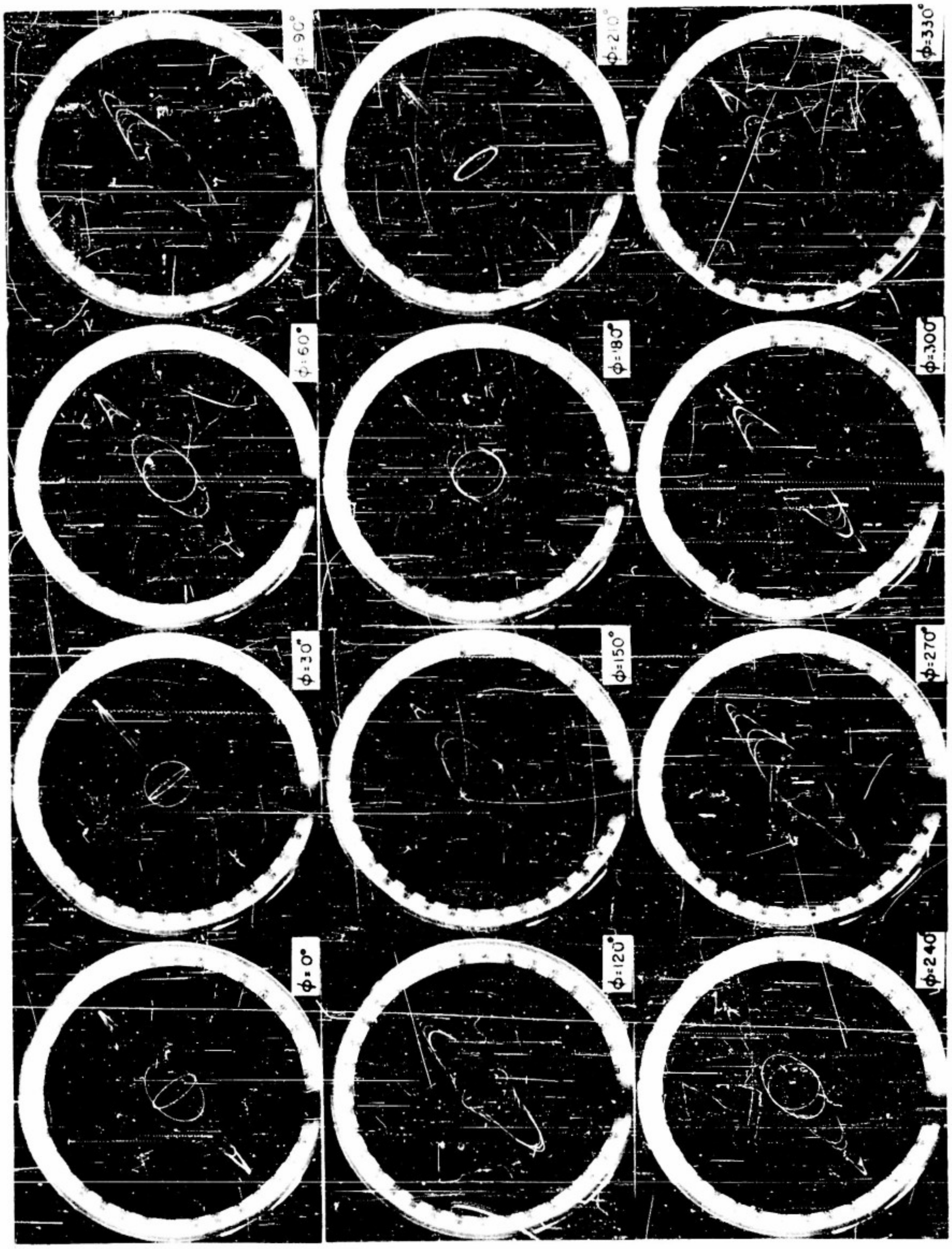

$B_1 = 35°$ $B_2 = 60°$ $h = 1.0$ $D = 5\lambda$ ϕ as indicated

COMPOSITE BEARING INDICATION OF A [illegible]-UNIT WADONAS

D=λ

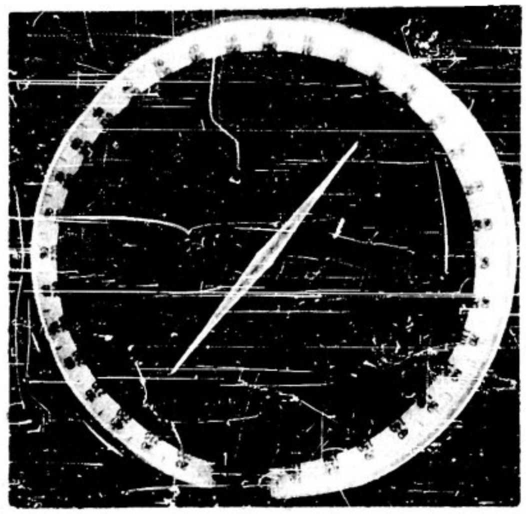

D=2λ

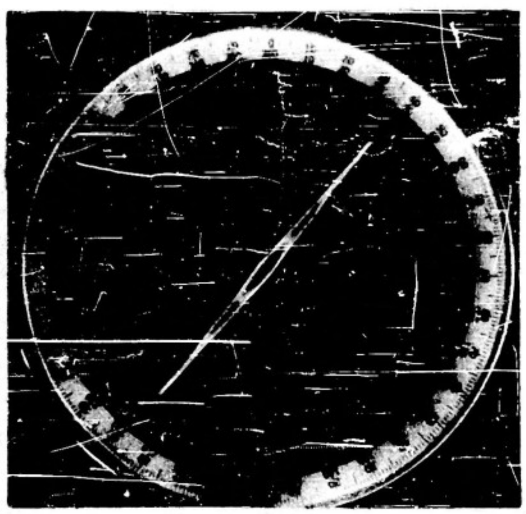

D=5λ

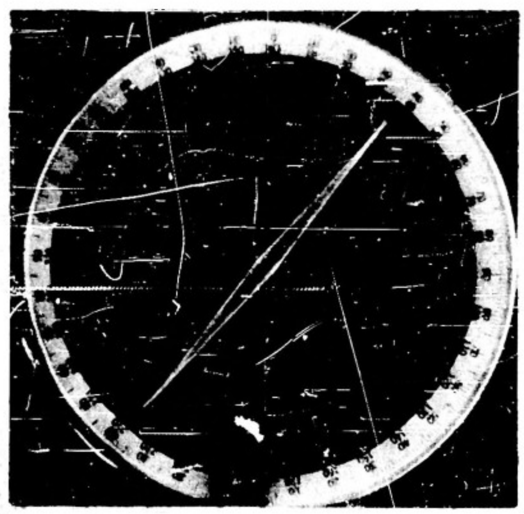

D=10λ

COMPOSITE BEARING INDICATION OF A 7--UNIT WADONAS FOR SPECIFIED APERTURES AND CONTINOUSLY VARYING ϕ

$B_1 = 35°$ $B_2 = 40°$ $h = 1.0$

DEPARTMENT OF ELECTRICAL ENGINEERING — UNIVERSITY OF ILLINOIS

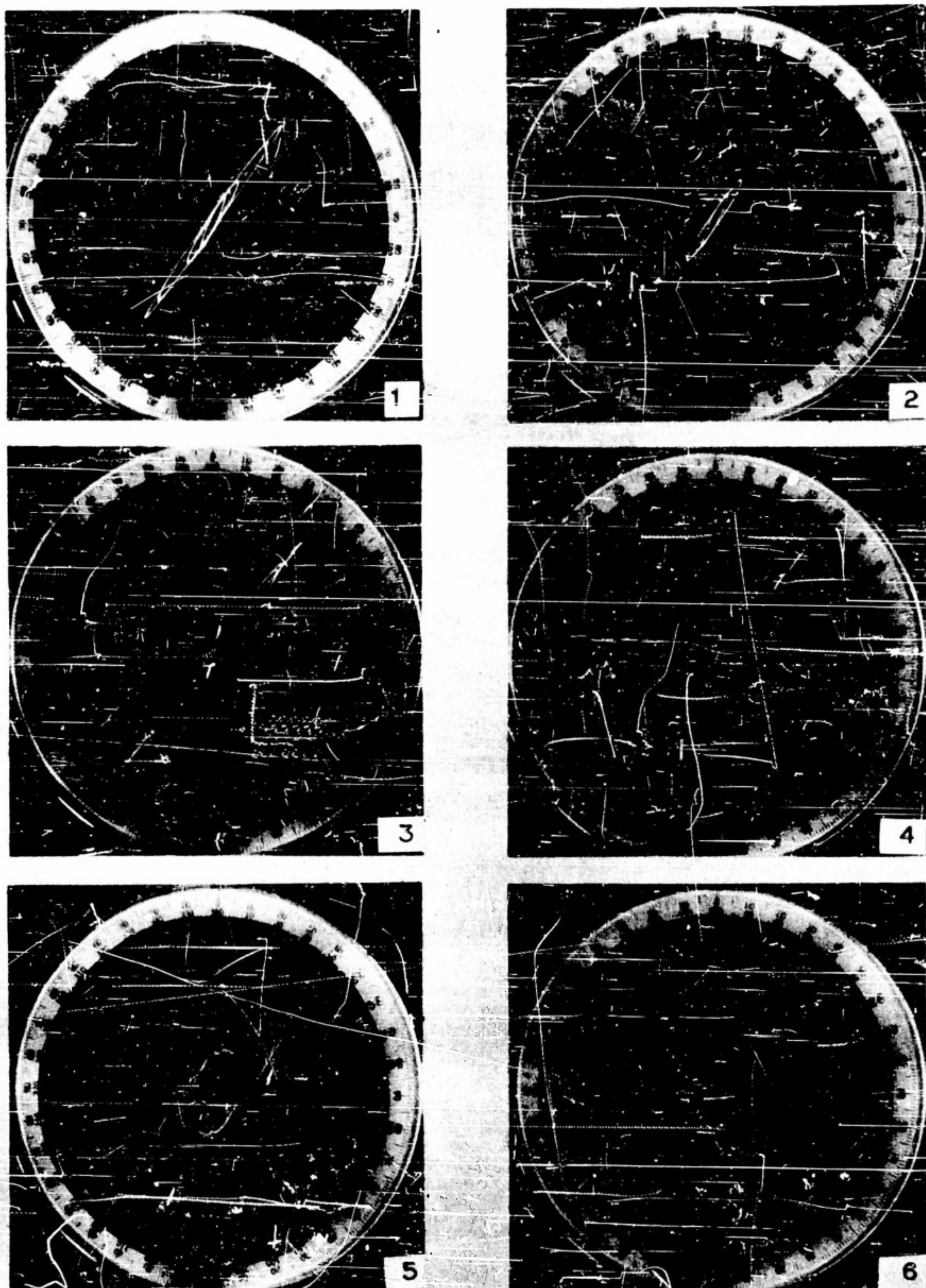

COMPOSITE BEARING AND SUPERIMPOSED OR DISPLACED ELECTRONIC CURSOR INDICATIONS OF A 7-UNIT WADONAS

$D = 5$ $h = 0.7$ $\theta_1 = 35°$ $\theta_2 = 40°$ (PHOTOS 1, 2)

$\theta_2 = 45°$ (PHOTOS 3,4) $\theta_2 = 60°$ (PHOTOS 5, 6)

DEPARTMENT OF ELECTRICAL ENGINEERING — UNIVERSITY OF ILLINOIS

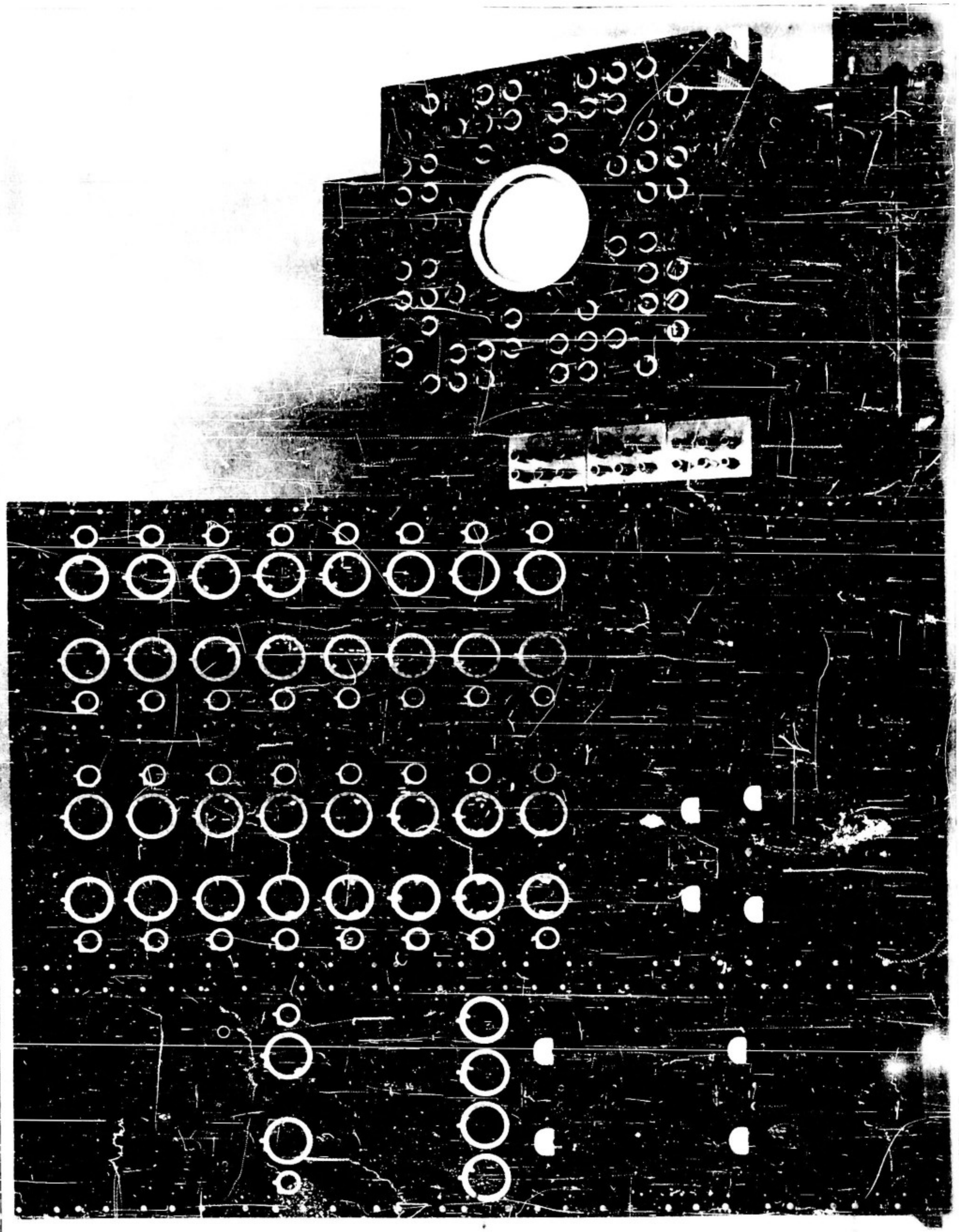

RDF SYSTEM ANALYZER AND EIGHT BEAM OSCILLOSCOPE

PLATE 17
TECH. REP 10

DEPARTMENT OF ELECTRICAL ENGINEERING — UNIVERSITY OF ILLINOIS

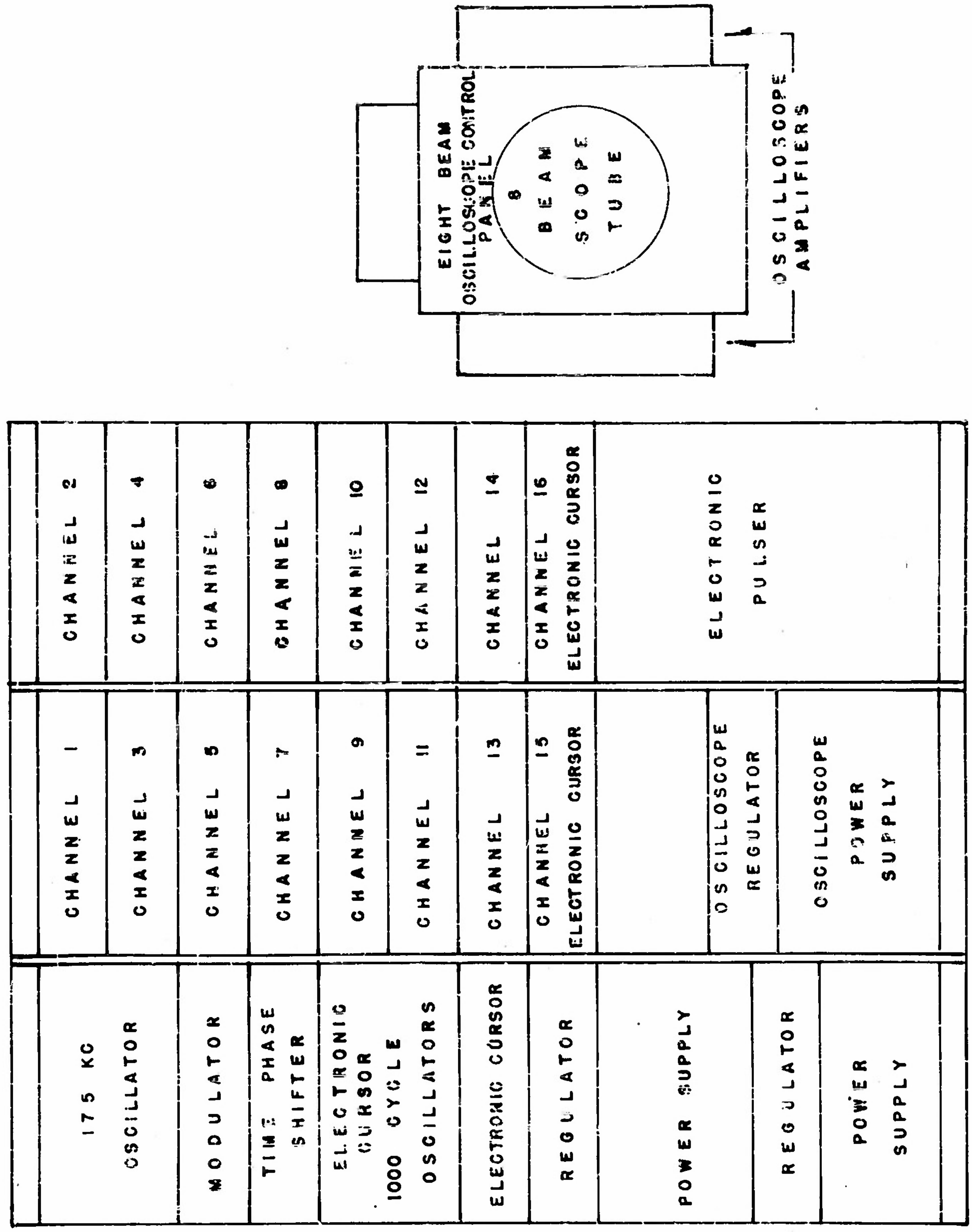

FIGURE 16

RDF SYSTEM ANALYZER AND EIGHT BEAM SCOPE

VIII. DISCUSSION OF PHOTOGRAPHS AND BEARING READING TECHNIQUES

An examination of the photographs of Section VII shows that, in general, the parallelogram-shaped envelope and, hence, the bearings of both arriving signals, can be fairly accurately determined. The technique of constructing an actual envelope with the aid of the electronic parallelogram cursor described in Appendix E is seen to be of considerable value in improving the accuracy of the determination.

Under favorable conditions, the parallelogram-shaped envelope is seen to give far more bearing information than a 'diversity' reading technique where the bearing is read from the longest ellipse corresponding to the strongest signal. However, if more than two incoming signals are present, the parallelogram-shaped envelope becomes a polygonal envelope with a number of parallel sides equal to twice the number of incoming signals. Each pair of sides is parallel to the direction of arrival of the particular incoming signal it represents and is of a length proportional to the strength of this signal. With only a restricted number of ellipses (for example, less than eight), it would be difficult or impossible to resolve the polygonal envelope for a large number of incoming signals (for example, more than four). Excessive noise or heavy modulation would complicate the problem still more. For such cases, it might be advisable to split the polygon (or pattern) along its major diagonal and estimate the best bearing by eye, if the direction of the longest side cannot be resolved. This would give about the same results as a diversity technique, either taking the bearing from the largest ellipse or by splitting the bearing between two large ellipses of equal size. With any of these techniques the guaranteed maximum bearing error for the WADONAS is far less than that for a single system.

Another special case needing consideration is that for two incoming signals of equal or nearly equal strength. Such cases would be almost certain to occur only when the angular separation is small (less than 20°), as they would result from split path (multipath) ionospheric transmission conditions. These conditions are the ones resulting in the worst errors - approaching 90° - for a single system. It can be seen from the photos that the bearing error for the WADONAS is not likely to exceed the angular separation. These is, however, some question as to which of any two equally large signals is the true bearing. Probably the best statistical approximation to the true bearing with only relative magnitude information available would be obtained by taking the angle half way between the arrival directions of two signals of equal strength. Hence, the best reading technique for the WADONAS would be to take the major diagonal of the parallelogram-shaped envelope.

Similarly, in the case of incoming signals having large relative magnitude (0.5 to 0.9), where the angular separation is small, (and split path transmission is indicated), the best bearing might be in between the bearings of the stronger and weaker signals, but closer to the stronger signal bearing than the weaker. Again such an intermediate bearing with exactly these characteristics is given by the major diagonal of the parallelogram. For intermediate values of relative magnitudes (0.3 to 0.7), with split path transmission, whether or not the longer side or the diagonal would give the best bearing cannot be answered with present day statistical information on propagation conditions. Other information, such as the relative time of arrival of the signals, might be more pertinent than relative magnitude considerations.* If the angular separation is large and/or back-scatter or site reradiation is indicated, then the longer side of the parallelogram would definitely give the best bearing.

* References (3) and (4)

IX. OPTIMUM APERTURES AND WIDE-BAND OPERATION

The photographs of Section VII give an indication of the minimum and maximum apertures which seem advisable to use, and, hence, give an indication of the range of possible operating frequencies for a WADONAS. Plate II clearly shows that for small angular separations ($\beta = 5°$) and the time phase $\varphi = 180°$, a system of 1 λ diameter is not large enough to give a large ellipse or an adequate bearing. Even two wavelengths diameter (Plate III, $\varphi = 180°$) is not too satisfactory, although it is a considerable improvement over one wavelength, and a tremendous improvement over a single system with $\beta = 5°$, and $\varphi = 180°$. Thus, it is seen that the lower limit for system diameter is determined by the necessity of producing ellipses with φ_n as far removed from the φ at the center as possible. As in nearly all wide-aperture systems, the required aperture will be a function of the angular separation, increasing as the angular separation decreases. More particularly, in order to produce a range of φ_n's deviating at most by ψ_{max} from the central φ, it is required that the diameter of the system (D) be at least:

$$D = \frac{\psi_{max}}{360 \sin \frac{\beta}{2}} \text{ wavelengths.} \tag{30}$$

This value is obtained as shown in the following discussion. It is shown in Appendix D that

$$\varphi_1 = \varphi - R \cos \Gamma_2 + R \cos \Gamma_1 \tag{31}$$

where R is the electrical radius in degrees. The time phase difference deviation from the center time phase difference, φ, will be called ψ.

$$\psi = R (\cos \Gamma_2 - \cos \Gamma_1). \tag{32}$$

From Figure D1

$$\Gamma_1 = \Gamma_2 + \beta \tag{33}$$

so that substituting equation (33) into (32) gives

$$\psi = R [\cos \Gamma_2 - \cos (\Gamma_2 + \beta)]. \tag{34}$$

Differentiate with respect to Γ_2 and set the derivative equal to zero to determine the maximum variation of ψ, ψ_{max}. This gives

$$\frac{\partial \psi}{\partial \Gamma_2} = R [\sin (\Gamma_2 + \beta) - \sin \Gamma_2] \tag{35}$$

from which

$$\sin (\Gamma_2 + \beta) = \sin \Gamma_2 . \tag{36}$$

Solutions of this equation are

$$\Gamma_2 = 90° - \frac{\beta}{2} ; \ 270° - \frac{\beta}{2}$$

which represent the maxima; the minima are not significant, as the quantity of interest is the absolute range of phase difference variation, either positive or negative. The maximum variation in the time phase difference will be found at a unit system position such that a line joining the unit system to the composite system center is perpendicular

to the bisector of the angle between the signals; i.e., $\Gamma_2 = 90° - \frac{\beta}{2}$.*
When $\Gamma_2 = 90° - \frac{\beta}{2}$ then, this maximum phase difference deviation ψ_{max} is

$$\psi_{max} = R\,[\cos \Gamma_2 - \cos (\Gamma_2 + \beta)]$$
$$= R\,[\cos (90° - \frac{\beta}{2}) - \cos (90° + \frac{\beta}{2})]$$
$$= 2R \sin \frac{\beta}{2}. \quad (37)$$

So that

$$D = 2R = \frac{\psi_{max}}{\sin \frac{\beta}{2}} \text{ in degrees}$$

$$= \frac{\psi_{max}}{360 \sin \frac{\beta}{2}} \text{ in wavelengths.} \quad (30)$$

Thus, for an angular separation of $\beta = 5°$, a diameter of about 1.9 wavelengths is required for $\psi_{max} = 30°$. For $\beta = 1°$, a diameter of 9.4 wavelengths is required for the same value of ψ_{max}.

Although a very small value of ψ_{max} would theoretically produce at least two ellipses adequate to determine the parallelogram envelope, examination of Plate III shows that it is sometimes difficult to determine the envelope with ψ_{max} less than 30° (D = 2λ for β = 5°). For ψ_{max} = 15° (D = 0.95λ for β = 5°) it becomes difficult even to form a general concept of the correct bearing if φ = 180°.

For excessively large apertures, a similar limit is imposed. When the aperture becomes large, the possibilities for the φ variations being nearly equal or differing by multiples of 360° are greatly increased. This tendency is roughly illustrated by Plate IV, φ = 0° where D = 5λ, and all of the ellipses except one are nearly coincident. At 5 and 10λ no conditions of exact coincidence were located as the photos show. If all were nearly equal and φ = 180°, then small ellipses and bad errors could result exactly as for the narrow-aperture systems. In the wide-aperture case, however, these effects would be more apt to occur with wide angles of separation where large relative magnitudes would not be as prevalent.

Thus, the lower limits on the system aperture would be expected to be more critical than the upper limits, and it would be advisable to keep the diameter above, at least, 2λ, extending it to as much as 20λ, if necessary.

A 20 to 2 wavelength range would mean that the system could be operated over a 10 to 1 frequency range (say 2 to 20 megacycles). This indicates that the useful bandwidth of the WADONAS is at least as good as that of the small aperture units currently available with which it would be constructed.

---

*Another way of arriving at this conclusion results from an examination of the interference field. (Reference 1)

X. CONCLUSIONS

It is concluded that seven Watson-Watt RDF units circularly distributed and connected so as to have optically superimposed bearing indications can form a system capable of completely resolving the directions of arrival of two signals under a majority of conditions. The distributed system is as nearly instantaneous as the units forming it. Under any conditions, the system is superior to diversity type of interconnections or a single Watson-Watt unit, especially in the case of flash transmissions. It is estimated that a 5λ aperture is roughly optimum, but that satisfactory operation over a range of 2 to 20λ is possible. It is further demonstrated that a system composed of a sufficient number of unit systems is theoretically capable of yielding the directions of arrival and relative magnitudes of any number of incoming signals. Finally it is to be noted that this system is equally capable of handling modulated signals inasmuch as the Watson-Watt units of which it is composed do not break down under conditions of modulated signal reception.

XI. BIBLIOGRAPHY

1. Summary Technical Report No. 4, University of Illinois, Direction Finding Research Laboratory, April 15, 1948.

2. Technical Report No. 7, "An Analysis of Radio Direction Finding Systems, Part 1," R. W. Annis, University of Illinois, Direction Finding Research Laboratory, September 1, 1948.

3. Technical Report No. 9, "A Comparison of Radio Direction Finding Systems," University of Illinois, Direction Finding Research Laboratory, December 1, 1949.

4. 'Multipath Propagation Effects in Direction Finding,' Report 5524, Hazeltine Ekectronics Corporation, May 10, 1950.

APPENDIX A

PROOF OF THE ELLIPTIC Z LOCUS

Equation (25) gives the locus of Z.

$$Z = A\,[\epsilon^{j\alpha}\cos\omega t + h\epsilon^{j(\alpha+\beta)}\cos(\omega t+\varphi)]. \tag{25}$$

Transforming this equation gives

$$Z = A\{(\cos\alpha + j\sin\alpha)\cos\omega t + h[\cos(\alpha+\beta) + j\sin(\alpha+\beta)]\cos(\omega t+\varphi)\}$$

$$= A\{[\cos\alpha\cos\omega t + h\cos(\alpha+\beta)\cos(\omega t+\varphi)] + j[\sin\alpha\cos\omega t + h\sin(\alpha+\beta)\cos(\omega t+\varphi)]\}. \tag{A1}$$

The X and Y coordinates of $\frac{Z}{A}$ are given as parametric functions of ωt:

$$X = \cos\alpha\cos\omega t + h\cos(\alpha+\beta)\cos(\omega t+\varphi) \tag{A2}$$

$$Y = \sin\alpha\cos\omega t + h\sin(\alpha+\beta)\cos(\omega t+\varphi). \tag{A3}$$

Let this be rearranged as follows

$$X = [\cos\alpha + h\cos(\alpha+\beta)\cos\varphi]\cos\omega t - h\cos(\alpha+\beta)\sin\varphi\sin\omega t \tag{A4}$$

$$Y = [\sin\alpha + h\sin(\alpha+\beta)\cos\varphi]\cos\omega t - h\sin(\alpha+\beta)\sin\varphi\sin\omega t \tag{A5}$$

This is of the form

$$X = k_1\cos\omega t - k_2\sin\omega t \tag{A6}$$

$$Y = k_3\cos\omega t - k_4\sin\omega t. \tag{A7}$$

Solving for $\sin\omega t$, $\cos\omega t$

$$\sin\omega t = \frac{\begin{vmatrix} k_1 & X \\ k_3 & Y \end{vmatrix}}{\begin{vmatrix} k_1 & -k_3 \\ k_2 & -k_4 \end{vmatrix}} = \frac{-k_3X+k_1Y}{-k_1k_4+k_2k_3} \quad \text{(A8)} \qquad \cos\omega t = \frac{\begin{vmatrix} X & -k_2 \\ Y & -k_4 \end{vmatrix}}{\begin{vmatrix} k_1 & -k_3 \\ k_2 & -k_4 \end{vmatrix}} = \frac{-k_4X+k_2Y}{-k_1k_4+k_2k_3}. \quad \text{(A9)}$$

Since $\sin^2\omega t + \cos^2\omega t = 1$

$$\left(\frac{-k_4X + k_1Y}{-k_1k_4+k_2k_3}\right)^2 + \left(\frac{-k_3X + k_1Y}{-k_1k_4+k_2k_3}\right)^2 = 1. \tag{A10}$$

Expanding and rearranging yields

$$(k_4^2+k_3^2)^2X^2 + (-2k_2k_4-2k_1k_3)XY + (k_2^2+k_1^2)^2Y^2 - (-k_1k_4+k_2k_3)^2 = 0. \tag{A11}$$

This of the form

$$AX^2 + BXY + CY^2 + DX + EY + F = 0 \tag{A12}$$

which is the standard equation of the general conic section. In this case D = E = 0. The equation represents an ellipse if $B^2-4AC < 0$. Set

$$B^2 - 4AC = R. \tag{A13}$$

Then

$$R = (-2k_2k_4-2k_1k_3)^2 - 4(k_4^2+k_3^2)(k_2^2+k_1^2) \tag{A14}$$

$$\frac{R}{4} = 2k_1k_2k_3k_4 - k_1^2k_4^2 - k_2^2k_3^2 \tag{A15}$$

$$-\frac{R}{4} = k_1^2k_4^2 - 2k_1k_2k_3k_4 + k_2^2k_3^2 \tag{A16}$$

$$+\frac{1}{2}\sqrt{-R} = k_1k_4 - k_2k_3 \tag{A17}$$

Since k_1, k_2, k_3, and k_4 are each entirely real, $\sqrt{-R}$ must be real, so that R must be negative. Thus, the equation (25) always represents an ellipse

APPENDIX B
INCLINATION OF THE ELLIPSE AND ERROR ANGLE

From analytic geometry, it is known that the inclination of the ellipse is given by θ where

$$\tan 2\theta = \frac{B}{A-C} . \tag{B1}$$

From Appendix A:

$$\tan 2\theta = \frac{-2k_2k_4-2k_1k_3}{k_4^2+k_3^2-k_1^2-k_2^2} . \tag{B2}$$

Inserting the values for the k's

$$\tan 2\theta = \frac{2\left\{\begin{array}{l}[\cos\alpha + h\cos(\alpha+\beta)\cos\varphi][\sin\alpha + h\sin(\alpha+\beta)\cos\varphi]\\ +[h\cos(\alpha+\beta)\sin\varphi][h\sin(\alpha+\beta)\sin\varphi]\end{array}\right\}}{\begin{array}{l}[\cos\alpha + h\cos(\alpha+\beta)\cos\varphi]^2 + [h\cos(\alpha+\beta)\sin\varphi]^2\\ -[\sin\alpha + h\sin(\alpha+\beta)\cos\varphi]^2 - [h\sin(\alpha+\beta)\sin\varphi]^2\end{array}}$$

$$= \frac{2\left\{\begin{array}{l}[\cos\alpha\sin\alpha + h\cos(\alpha+\beta)\cos\varphi\sin\varphi\\ +h\sin(\alpha+\beta)\cos\varphi\cos\alpha + h^2\cos(\alpha+\beta)\sin(\alpha+\beta)]\end{array}\right\}}{\begin{array}{l}\cos^2\alpha + 2h\cos\alpha\cos\varphi\cos(\alpha+\beta) + h^2\cos^2(\alpha+\beta)\\ -\sin^2\alpha - 2h\sin\alpha\sin(\alpha+\beta)\cos\varphi - h^2\sin^2(\alpha+\beta)\end{array}}$$

$$= \frac{\sin 2\alpha + 2h\cos\varphi\sin(2\alpha+\beta) + h^2\sin 2(\alpha+\beta)}{\cos 2\alpha + 2h\cos\varphi\cos(2\alpha+\beta) + h^2\cos 2(\alpha+\beta)} . \tag{B3}$$

Hence, the angle of inclination of the major axis of the ellipse with respect to the X axis is given by

$$\theta = \frac{1}{2}\tan^{-1}\frac{\sin 2\alpha+2h\cos\varphi\sin(2\alpha+\beta) + h^2\sin 2(\alpha+\beta)}{\cos 2\alpha+2h\cos\varphi\cos(2\alpha+\beta) + h^2\cos 2(\alpha+\beta)} . \tag{B4}$$

To find the error angle θ_e, which is the angle between the major axis of the ellipse and the direction of arrival of Wave 1, it is merely necessary to set $\alpha = 0$ in the above expression. This yields

$$\theta_e = \frac{1}{2}\tan^{-1}\frac{2h\sin\beta\cos\varphi + h^2\sin 2\beta}{1 + 2h\cos\beta\cos\varphi + h^2\cos 2\beta} . \tag{B5}$$

In Fig. 3 is shown the construction for θ_e when $\varphi = 0$. This gives

$$\tan\theta_e = \frac{h\sin\beta}{1 + h\cos\beta} . \tag{B6}$$

To show that this is equivalent to the expression just derived for θ_e at $\varphi = 0$, rearrange equation (B5) and set $\varphi = 0$, then

$$\tan 2\theta_e = \frac{2h\sin\beta + h^2\sin 2\beta}{1 + 2h\cos\beta + h^2\cos 2\beta} . \tag{B7}$$

Now:

$$\tan 2\theta_e = \frac{2 \tan \theta_e}{1 - \tan^2\theta_e} \quad . \tag{B8}$$

Using:

$$\tan \theta_e = \frac{h \sin \beta}{1 + h \cos \beta} \tag{B6}$$

then

$$\tan^2 \theta_e = \frac{h^2 \sin^2 \beta}{(1 + h \cos \beta)^2} \tag{B9}$$

$$1-\tan^2\theta_e = 1-\frac{h^2 \sin^2 \beta}{(1+h \cos \beta)^2} = \frac{(1+h \cos \beta)^2-h^2 \sin^2 \beta}{(1+h \cos \beta)^2} = \frac{1+2h \cos \beta+h^2 \cos 2\beta}{(1+h \cos \beta)^2} \tag{B10}$$

and

$$\tan 2\theta_e = \frac{2 \tan \theta_e}{1-\tan^2\theta_e} = \frac{\dfrac{2h \sin \beta}{1+h \cos \beta}}{\dfrac{1+2h \cos \beta+h^2 \sin 2\beta}{(1+h \cos \beta)^2}} = \frac{2h \sin \beta(1+h \cos \beta)}{1+2h \cos \beta+h^2 \sin 2\beta}$$

$$= \frac{2h \sin \beta+h^2 \sin 2\beta}{1+2h \cos \beta+h^2 \sin 2\beta} \tag{B11}$$

and the equivalence is shown.

APPENDIX C

DEVELOPMENT Z LOCUS FOR THREE SIGNALS

In Section IV, equation (25) for the Z trace of the Watson-Watt system for the case of one interfering wave is derived. As the electric fields due to any number of arriving waves linearly superimpose themselves at the antennas, the contribution of the field caused by each wave to an antenna differential voltage is of the form

$$e_x = 2h_n e_0 r K \cos(\alpha+\beta_n)\cos(\omega t+\varphi_n) \qquad (C1)$$

where h_n, β_n, φ_n, are the relative magnitudes, deviations in arrival directions, and relative time phases, respectively, of the nth wave, all measured with respect to Wave 1. The trace of the oscilloscope beam due to n arriving waves is given by

$$Z = A[\epsilon^{j\alpha}\cos\omega t+h_1\epsilon^{j(\alpha+\beta_1)}\cos(\omega t+\varphi_1) + h_2\epsilon^{j(\alpha+\beta_2)}\cos(\omega t+\varphi_2) + \cdots +h_n\epsilon^{j(\alpha+\beta_n)}\cos(\omega t+\varphi_n)] \qquad (C2)$$

or

$$Z = A\,\epsilon^{j\alpha}\sum_{m=0}^{n} h_m\,\epsilon^{j\beta_m}\cos(\omega t+\varphi_m), \qquad (C3)$$

where $h_0 = 1$.

The indication resulting from the WADONAS due to more than one interfering signal is readily visualized. The envelope of the Z loci is a polygon having a pair of sides corresponding to each signal present, the lengths and the inclination of the pair of sides being proportional to the relative magnitude and direction of arrival of that particular signal.

An argument identical to that given earlier for the case of two waves shows that for three waves, one has

$$Z = A[\epsilon^{j\alpha}\cos\omega t+h_1\epsilon^{j(\alpha+\beta_1)}\cos(\omega t+\varphi_1)+h_2\epsilon^{j(\alpha+\beta_2)}\cos(\omega t+\varphi_2)] \qquad (C4)$$

and the envelope of the loci is a six-sided figure, shown in Fig. C1 for the h's and β's listed. Wave 1 is considered to be the desired wave and the other two might be due to extra-length path transmission. As in the case of two signals, one is again able to separate the components of the field strength both in magnitude and direction provided there is a distribution of narrow-aperture systems such as to produce a satisfactory distribution of relative time phase values.

Figure C2 is a photograph of the envelope of the Z loci for three signals. The photograph was obtained on the antenna simulator for the particular case where wave 1 arrives from a bearing of +20° azimuth. Wave 2 bears 15° counter clockwise from wave 1 and has a relative amplitude of 0.9. Wave 3 bears 30° clockwise from wave 1 and has a relative amplitude of 0.7. The time phases of waves 2 and 3 relative to wave 1 are varying. It is seen that the actual photograph bears out the three-signal theory stated above.

The shape of the envelope of the Z loci for more than three signals present follows by induction from the foregoing.

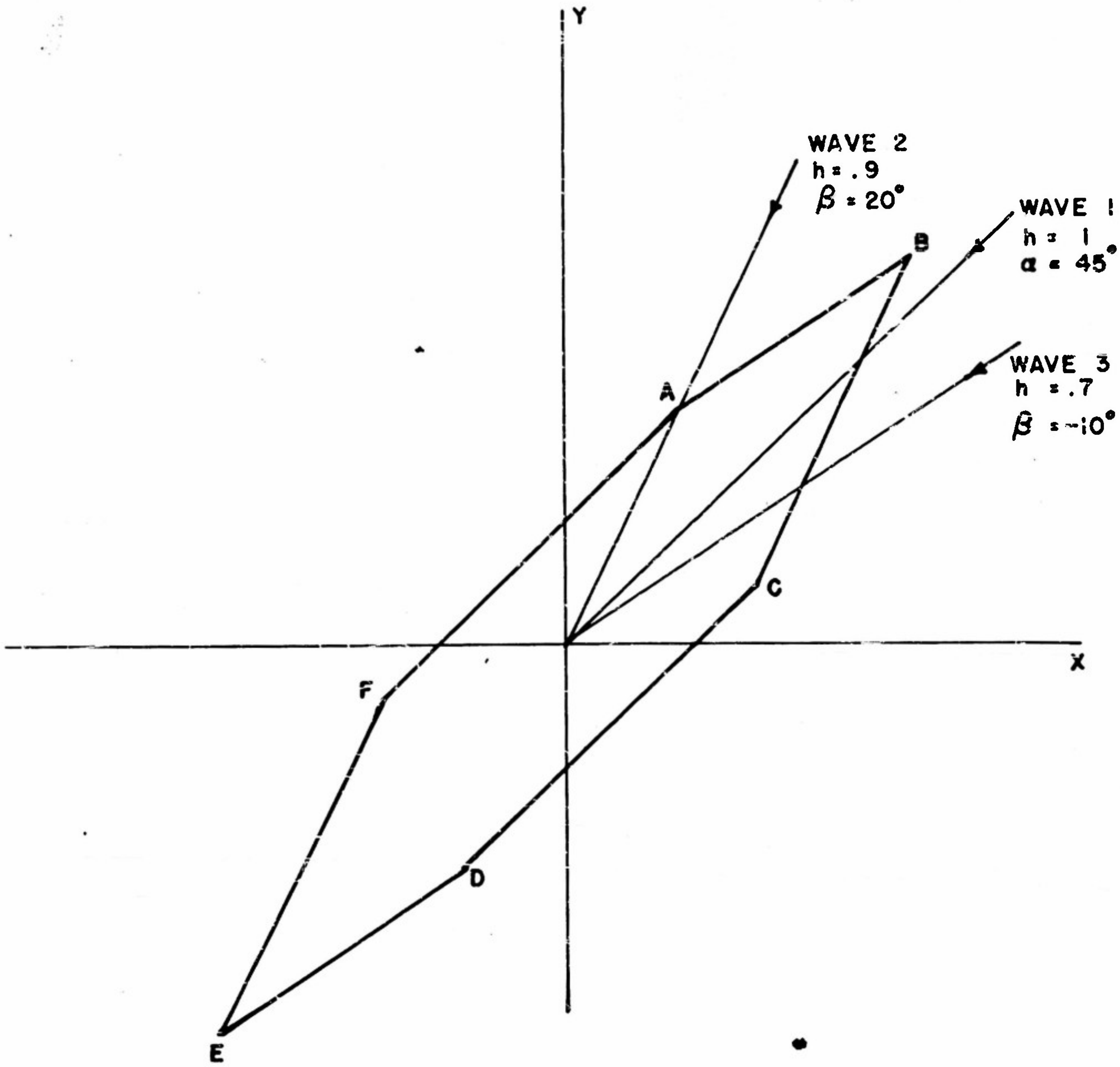

FIGURE C1

ENVELOPE OF THE Z LOCI FOR 3 SIGNALS

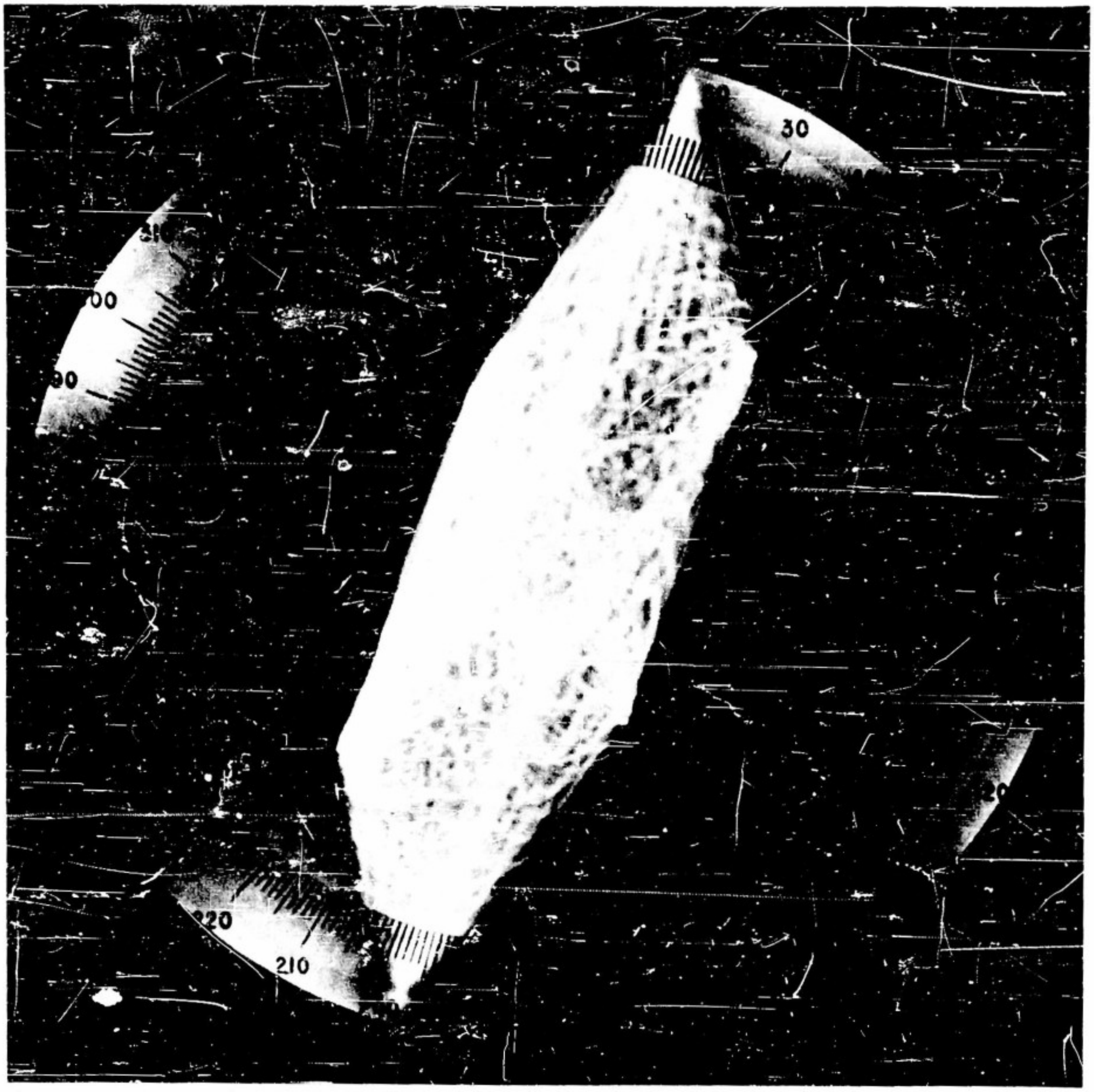

WAVE 1	h = 1.0	α = 20°
WAVE 2	h = 0.9	β = -15°
WAVE 3	h = 0.7	β = + 30

FIGURE C2

ENVELOPE OF THE Z LOCI FOR 3 SIGNALS

APPENDIX D
DEVELOPMENT OF φ_n

The explanation for the time phase difference between the desired and undesired signals varying from system to system when the systems are widely separated can be seen from an examination of the interference field as pictured in Plate 1 of Technical Report 4. To obtain a more exact picture for the case of two systems at random location with respect to two incoming signals, examine Fig. D1. Let the two systems be on the periphery of a circle of radius R in electrical degrees (corresponding to a particular wavelength for the incoming signals). Let the time phase difference between the signals at the center of this circle be φ, and let φ_1 and φ_2 be the time phase difference between the desired and undesired signals at the center of unit systems (Watson-Watts) 1 and 2, respectively. Now let the field at the center of the circle due to the desired signal be

$$E_m \cos \omega t \tag{D1}$$

and the field at the center of the circle due to the undesired signal be

$$E_m \cos (\omega t+\varphi) \tag{D2}$$

Then, the field at the center of system 1, resulting from the desired signal is

$$E_m \cos (\omega t-R \cos \Gamma_1) \tag{D3}$$

and the field at the center of system 1 resulting from the undesired is

$$h\ E_m \cos(\omega t+\varphi-R \cos \Gamma_2) \tag{D4}$$

Hence, φ_1, can be expressed as

$$\varphi_1 = (\varphi-R \cos \Gamma_2+R \cos \Gamma_2). \tag{D5}$$

Similarly, the field at the center of system 2 resulting from the desired signal is

$$E_m \cos(\omega t- R \cos \Gamma_4) \tag{D6}$$

and from the undesired signal is

$$h\ E_m \cos(\omega t+\varphi- R \cos \Gamma_3). \tag{D7}$$

Hence, φ_2, can be expressed as

$$\varphi_2 = (\varphi- R \cos \Gamma_3+ R \cos \Gamma_4); \tag{D8}$$

and since Γ_1, Γ_2, Γ_3, and Γ_4 are generally independent for randon locations of systems 1 and 2, φ_1 is generally different from φ_2.

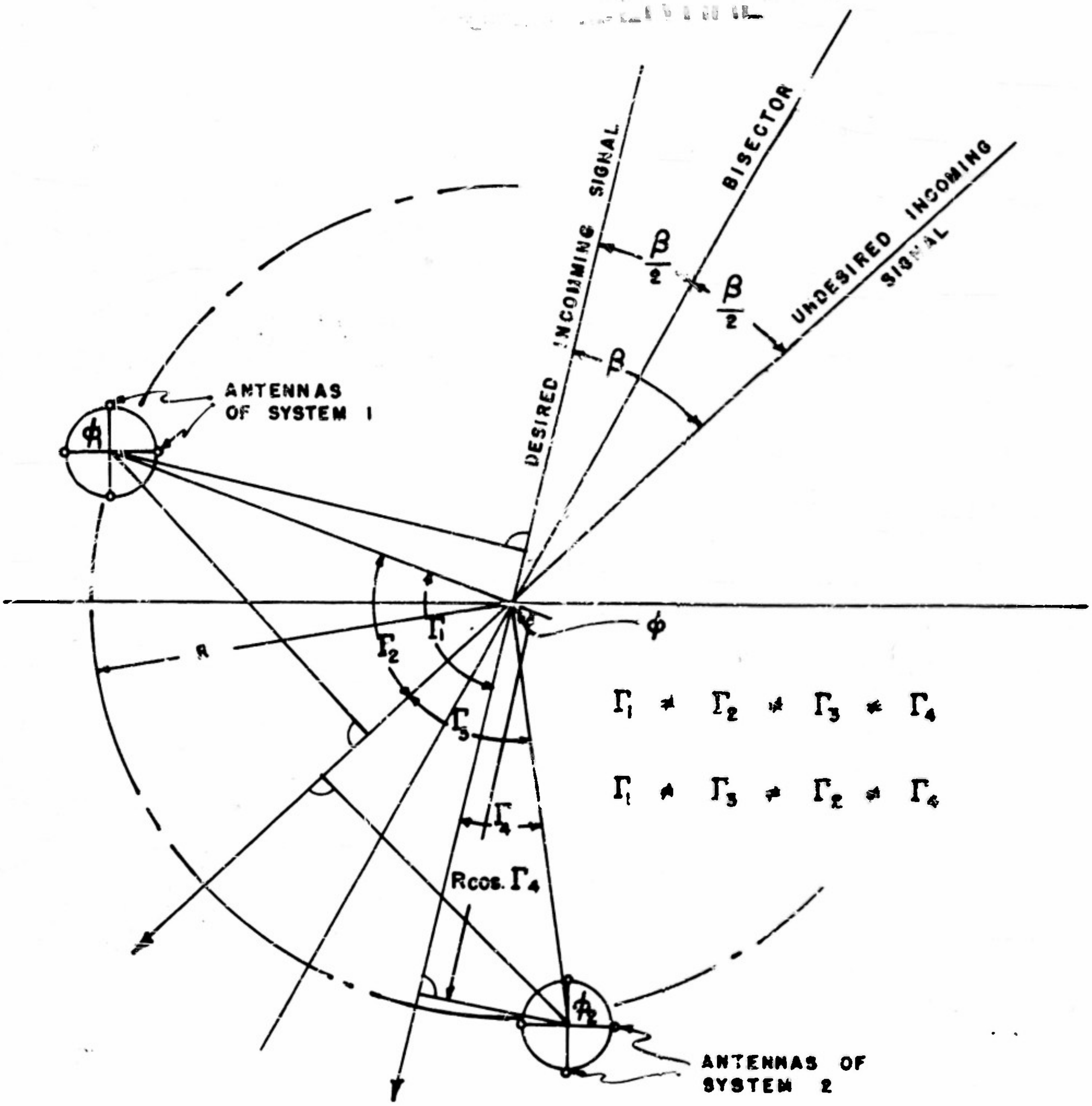

FIGURE DI

TIME PHASE DIFFERENCE AT THE CENTER OF A UNIT SYSTEM AS A FUNCTION OF ITS LOCATION IN THE INTERFERENCE FIELD

CONFIDENTIAL

UNCLASSIFIED

UNCLASSIFIED